Thesis for the Degree of Master of Science

Comparative Analysis of HD Diesel Engine with & without Humidification at low load operation

Evgeny Orlov

LUND UNIVERSITY

ISRN LUTMDN/TMHP-15/5345-SE

Department of Energy Sciences

Division of Combustion Engines

LTH

Lund, Sweden 2015

Abstract

High fuel prices and stringent emission norms stimulate the improvement of engine efficiency and emission reductions. This is one of the leading issues in the truck industry. A waste heat recovery technology (WHR) can be used to solve this issue. The evaporative cycle represents the WHR.

This thesis is part of a research project which is carried out at the department of Energy Science at Lund University. Comparative analysis of a HD Diesel Engine with and without humidification is studied in this project. The aim of the project is to reduce local emissions (NOx, HC, PM and CO) and improve fuel consumption efficiency. Humid Air Motor known as HAM is a technology originally invented in Lund University and this technology has certainly succeeded in a marine engine. The major benefit of the HAM is the sufficient reduction of the emissions, while there is no deep understanding of the efficiency process. The main idea of this project is to test the HAM concept on a heavy duty truck diesel engine.

A major part of the project is to perform experimental work on a HD Volvo truck diesel engine. Also, studies on the Rankine cycle at an advanced level, simulations in the GT-Power software, making the thermodynamic model of the humidification tower etc. are also included. The goal of this project is to investigate the effectiveness of the HAM system and to compare the results with conventional diesel engines with and without EGR cooler.

Acknowledgements

There are many people to thank for this thesis finally being written. First of all I would like to thank my supervisor, Martin Tunér, who gave me the opportunity to perform this thesis at the Division of Combustion Engines and the valuable meetings during the whole work at the department.

I also want to give a special thanks to Prakash Narayanan, my daily supervisor, who helped me a lot and supported me all the way. He always had time to help me and explained everything that I did not really understand very well. Big thanks!

Last, but absolutely not least, I would like to thank Professor Per Tunestål, who examined my report and helped me and Prakash with different problems during the experimental work. Thanks to Professor Bengt Johansson who always gave a good piece of advice. Thanks also to Sam and Nhut, who were helpful and the laboratory technicians, who helped to get the HAM system started. And thanks to Gustav and Jonathan for making this time here very pleasant and fun.

Nomenclature

ATDC	After Top Dead Center
BMEP	Brake Mean Effective Pressure
CAD	Crank Angle Degree
CDC	Conventional Diesel Engine
EGR	Exhaust Gas Recirculation
FSN	Smoke Number
HAM	Humid Air Motor
HRR	Heat Release Rate
HT	Humidification Tower
IMEPg	Gross Indicated Mean Effective Pressure
IMEPn	Net Indicated Mean Effective Pressure
LHV	Lower Heating Value
NOx	NO and NO2
Pin	Inlet Pressure
PM	Particulate Matter
SOI	Start Of Injection
Tin	Inlet Temperature
VGT	Variable-Geometry Turbocharger

Table of Contents

Chapter 1

Introduction

This thesis work has been carried out at the Division of Combustion Engines within the Faculty of Engineering of Lund University. It is a part of the HAM project, which is described in this chapter.

1.1 Background

The internal combustion engine has had a major impact on our society through improved industrial and transport sectors. The invention of the combustion engine was one of the biggest turning points in our history [3]. In 1680, Christian Huygen was the first who experimented with an idea of the internal combustion engine. Later on, in 1876, Nikolaus Otto created a successful four-stroke engine known as the "Otto cycle". It was the first internal combustion engine that compressed the fuel mixture prior to combustion. Back then, this engine had the highest thermal efficiency [1].

In 1898, another internal combustion engine was built by Rudolf Diesel. This engine had the highest thermal efficiency of any standard internal combustion engine because of its very high compression ratio. Diesel engines have continuously been under development and still are [2].

Evolution in the automobile history took place worldwide. It was the long way to produce the modern automobile and it is estimated that over 100 000 patents have been done to create the modern car. German engineer, Karl Benz, designed and built the world's first practical car in 1885 and Henry Ford improved the assembly line for car manufacturing. The first steam, electrical and gasoline engine cars started the history of automobiles [3].

In the beginning of car manufacturing, the focus was on exterior styling, durability and performance of cars. Nowadays the focus has shifted to developing modern combustion engines that reduce emissions and fuel consumption. The increase in fuel prices and stringent emission norms forced the automotive and truck industry to find new ways and technologies to reduce fuel consumption.

1.1.1 Engines today

Nowadays society is highly dependent on transportation by trains, cars, airplanes and others. All of the transportation means have an effect on global warming. The transport sector takes one fourth part of the total energy use in Sweden and it represented 33 % of the greenhouse gas emissions in 2012 [5]. According to statistics from the Traffic Analysis, the number of diesel cars almost quadrupled in 10 years. In 2012, diesel cars accounted for 60% of new car registrations in Sweden. In spite of using diesel engines for passenger cars, an enormous amount of diesel engines for heavy

traffic cars and busses were used. The situation with heavy duty engines in other countries is the same [4].

Emission norms raise the bar for greenhouse gases higher and higher. In order to satisfy these norms it forces the truck industry to find new technologies for reducing emissions from diesel and petrol vehicles. Trends of worldwide emission standards are shown in Figure 1.1. For the last seventeen years, emission norms became tougher and greenhouse gas emissions were sufficiently decreased. The reduction of gases started with the Euro 0 and now the Euro 6 is the permitted standard for emissions.

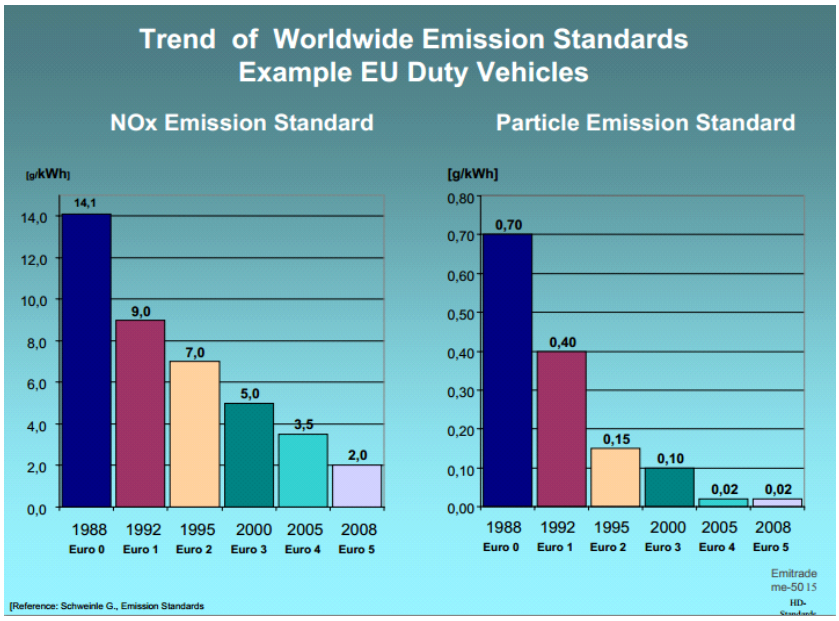

Figure 1.1 Trend of worldwide emission standards [6]

Fuel prices increase almost every year, it can be seen in Figure 1.2. Efficiency improvement is important for the truck industry if high demand for diesel engines is to be kept. Even the decrease of oil prices keeps the fuel prices almost constant in Sweden.

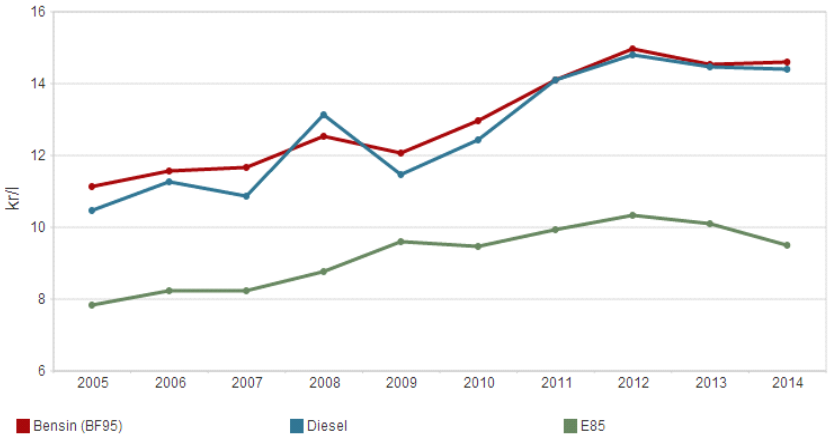

Figure 1.2 Selling price development of petrol, diesel and ethanol [7]

1.2 Internal combustion engines

The internal combustion engine is a heat engine with internal combustion. Natural gas, petrol or diesel are the main fuels which can be used for combustion. There is also a growing usage of renewable fuels. For example, bioethanol for spark ignition engines and biodiesel for compression ignition engines [8]. The internal combustion engines can be divided into a few groups and the three most significant are spark-ignition, compression-ignition and homogeneous charge compression ignition engines. Each group can be found in four-stroke and two-stroke variants [9]. All groups have the same principle for the engine cycle, which is shown in Figure 1.3 for the four-stroke spark ignition engine. This engine cycle has the following strokes: (a) intake, (b) compression, (c) power/expansion and (d) exhaust. The expansion stroke is responsible for the work done by the engine.

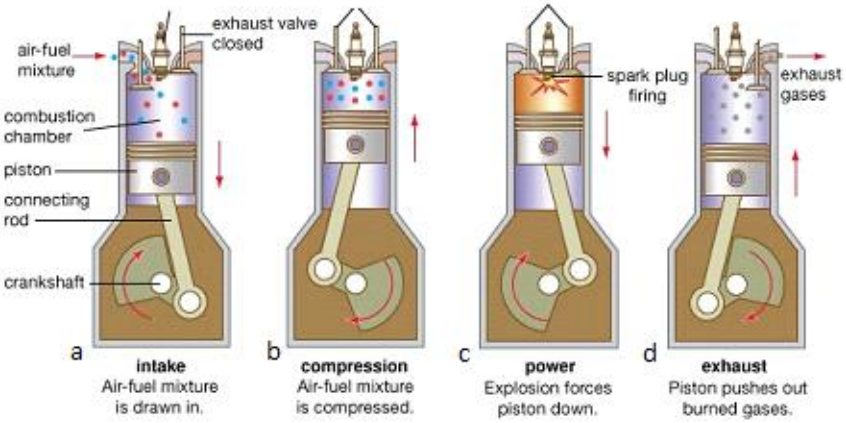

Figure 1.3 The four-stroke cycle [10]

1.3 Diesel engines

A compression-ignition engine is a diesel engine with internal combustion. The working procedure for diesel engine begins with clean air being compressed during the compression stroke. The heat of compression is used to initiate ignition and the fuel is injected with high pressure into the combustion chamber at the end of the compression stroke. Compressed air has very high temperature that makes the fuel ignite instantaneously when it is injected into the cylinder. Diesel engines have lower fuel consumption compared to other internal combustion engines. This advantage keeps diesel engines being high in demand [11].

1.3.1 Combustion process in the diesel engine

The diesel engine combustion process is represented in Figure 1.4 and can be divided into three parts, namely heat release in three steps [12]:

- Ignition Delay
- Premixed Combustion
- Mixing-Controlled Combustion

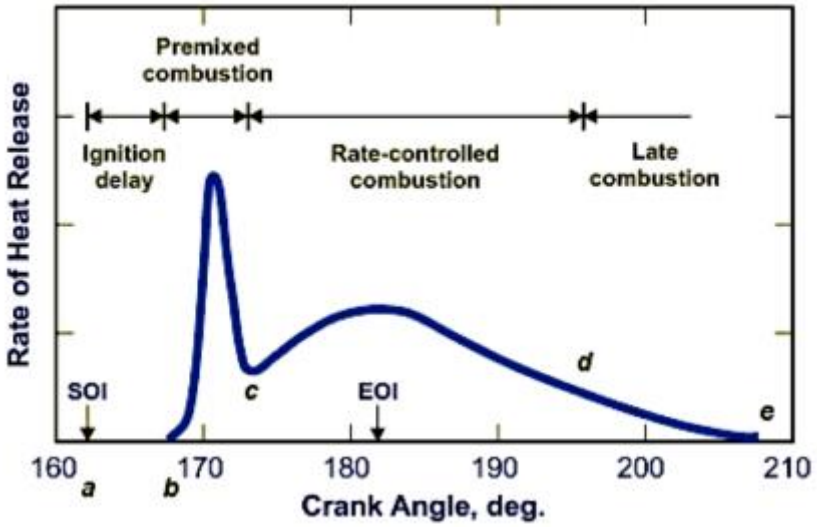

Figure 1.4 Heat release for conventional diesel engine [29]

(a-b) is the ignition delay period between the start of injection and start of combustion, depending on the temperature in the cylinder, fuel quality and fuel injection velocity. The air-fuel mixture has to reach a temperature above 800 K for ignition to occur.

(b-c) is the premixed combustion phase, showing the spontaneous ignition at one or more locations in the cylinder. Combustion starts if local stoichiometry and amount of fuel-air mixture are right in some regions of the cylinder. Temperature and pressure will rapidly increase in the cylinder which causes spontaneous ignition in other regions. The amount of heat released depends on the amount of fuel injected into the cylinder and in turn this determines how much the pressure will increase.

(c-d) is the mixing-controlled combustion phase, the quasi-steady diffusion combustion, where most of the heat release takes place. This quasi-steady process means that the fuel is injected and is then atomized followed by mixing with air and burned continuously. The process does not change adequately with time [12].

1.4 Emissions

The amount of pollution that cars and trucks emit depends on many factors. Computer models are used to estimate the average emissions for different types of vehicles. Six common air pollutants are: CO2, nitrogen oxides (NOx), Ozone, CO, Particulate matter (PM10 and PM2.5) and Sulfur Dioxide (SO2). Heavy duty vehicle produces about a quarter of CO2 emissions in EU. This represents 5 % of the EU's total greenhouse gas emissions [13].

Approximately 60% of nitrogen oxides emissions in Sweden are from diesel vehicles. Heavy and light trucks represent about 20 % each, 12 % are represented by cars and 5 % by buses. Passenger cars that are powered by petrol represent 25 % of NOx emissions in Sweden [14].

The amount of emissions per work done (specific emissions), can be calculated if the EI (emissions index) is known. The EI is the amount of emissions per amount of fuel.

$$sX = \frac{\dot{m}_x}{P} = \frac{\dot{m}_x}{\dot{m}_f} * \frac{\dot{m}_f}{P} = \frac{EI_x}{1000} bsfc \quad (1.1)$$

$\dot{m}_f$ is the fuel flow, *X* is the exhaust gas and $\dot{m}_x$ is the exhaust gas flow. *bsfc* (specific fuel consumption) and *sX* (specific emissions) are given in g/kWh.

$$bsfc = \frac{\dot{m}_f}{P} \quad (1.2)$$

Where P is power and EI_x is the emission index.

$$EI_x = \frac{\dot{m}_x}{\dot{m}_f} * 1000 \quad (1.3)$$

The decrease of fuel consumption make specific emissions decrease and that is why it is important to improve the efficiency of the engine [11].

1.4.1 Diesel emissions

HC, NOx, PM (especially soot) and CO are the most common pollutant emissions from diesel engine. Relative concentration of pollutant emissions in diesel exhaust gas is presented in Figure 1.5. A very big part of the diesel exhaust gases is nitrogen gas as can be seen in the figure [15].

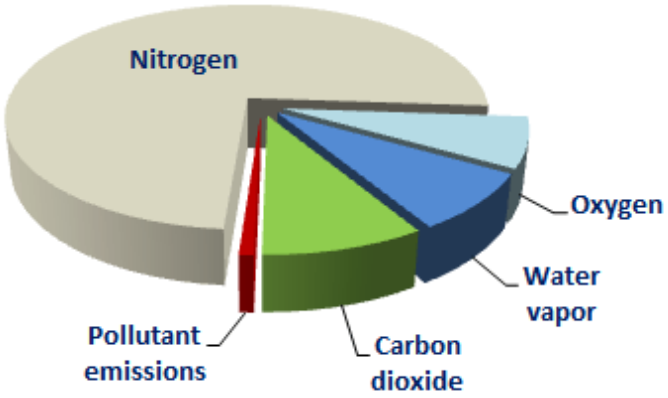

Figure 1.5 Relative Concentrations of Pollutant Emissions in Diesel Exhaust Gas [15]

Diesel vehicles barely emit CO emissions because of the lean combustion process and low fuel consumption but release large quantities of NOx and PM.

Figure 1.6 shows a model for diesel combustion under the latter part of diesel combustion. Air mixes with fuel and forms a rich mixture. This mixture burns in a fairly thin premixed flame marked with blue color. Soot formation is marked with gray color, because of the rich combustion. Those little particles increase in size and amount, as they are transported downstream. Oxidation of soot and combustion of rich products occurs at the thin diffusion flame. Thermal NOx production zone is narrow due to the necessity of oxygen and high temperature at the same time.

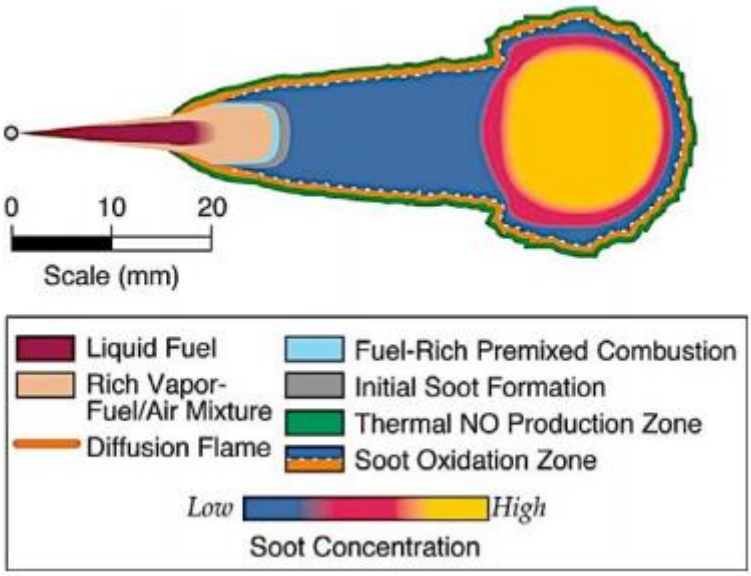

Figure 1.6 Modell for diesel combustion under the latter part of combustion [30]

1.4.1.1 NOx

NOx is a mixture of oxides of nitrogen comprising NO and NO_2. There are three primary sources of NOx in combustion processes: thermal, prompt and nitrous oxide. Thermal NOx tends to dominate during the combustion and it is highly temperature dependent. Thermal NOx formation reactions described by the Zeldovich and Lavoie are following [28]:

$$N_2 + O = NO + N \quad (1.4)$$

$$N + O_2 = NO + O \quad (1.5)$$

$$N + OH = NO + H \quad (1.6)$$

All reactions are reversible and NO concentration is higher at higher temperatures. There is high NOx formation at early phased combustion because of high temperature and low engine-out NOx concentration at late phased combustion.

NOx is formed in warm and available oxygen zones, where oxygen is found in exuberance, i.e. in lean mixtures at high temperatures. For lean mixtures lambda is more than 1. Normalized *air/fuel-ratio* is lambda [11].

$$\lambda = \frac{A}{F} / (\frac{A}{F})_s \quad (1.7)$$

$\frac{A}{F}$=*air flow/fuel flow.* $(\frac{A}{F})_s$ is the ideal stoichiometric ratio.

Variation of load shows that the Emission index (EI) increases with the load decrease. With the load decreased, more and more combustion in the premixed combustion part occurs while the amount of oxides of nitrogen (NOx) increases per unit of fuel [11].

1.4.1.2 Particulate matter (PM)

Particulate matter comes from the very heterogeneous combustion (diesel combustion). PM consists substantially of coal which is called soot. Soot particles are the largest components of PM emissions. In the latter part of the expansion stroke and in the exhaust system, soot can absorb different hydrocarbons. These hydrocarbons are dangerous and highly cancerogenic [18].

Soot (smoke) forms in rich mixtures with lack of oxygen and forms in premixed combustion part. Big part of soot will be oxidized under the latter part of the combustion process. It depends on the pressure and temperature cycle. High temperatures give high oxidation of soot. Approximately 90 % of soot will be consumed before the expansion stroke is over. Then the amount of fuel increases and comes near the stoichiometric mixture, soot oxidation will be more difficult which is why more soot is formed in rich mixtures [11]. This restriction of air utilization is the main reason for the diesel engines' deficiency of delivering as much power as a petrol engine, which performs it at the same conditions. However, there are always two sides of the coin as the diesel engine consumes less fuel per kilometer, while the petrol engine has higher thermal efficiency per unit fuel [33].

1.4.1.3 Hydrocarbons (*HC)*

Incomplete combustion of fuel is the main reason for hydrocarbons emissions. HC has negative effects on human health and is very toxic. Lean air to fuel ratios can reduce HC emissions [17].

1.4.2 Methods of reducing NOx and PM emissions

The recycling of the exhaust gas (EGR) and selective catalytic reduction (SCR) are the main methods of reducing NOx.

EGR is the recycling of exhaust gas which cools down and sends part of the exhaust gas back into the combustion chamber of the diesel engine. This exhaust gas mixes with intake air before coming into the combustion chamber and thereby the combustion temperature is reduced [19].

There are some disadvantages with the EGR process, namely [20]:

- Increase in fuel consumption
- Production of particulates (PM) will increase because of less access to the oxygen
- Peak power available from the engine will be reduced because of the reduction of available oxygen in the cylinder and extra pumping
- The EGR stream needs extra cooling and pumping

Figure 1.7 represents trade-off between NOx and soot for a diesel engine. Figure shows that NOx is reduced but at the expense of soot and fuel consumption. NOx reduction increases soot formation and fuel consumption [21].

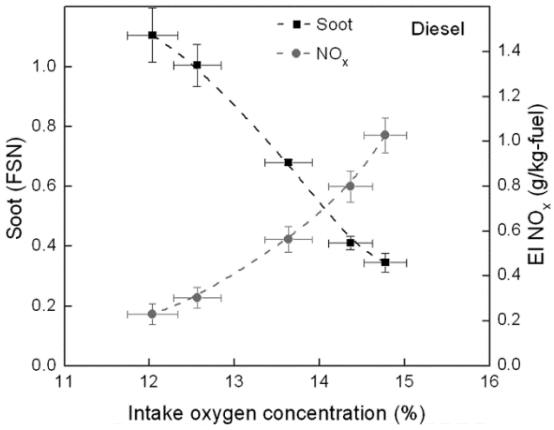

Figure 1.7 Trade-off between NOx and soot for a diesel engine [31]

Catalyzed diesel particulate filter (CDPF) and diesel oxidation catalyst (DOC) are the most common PM emissions reduction technologies for diesel engines. CDPF is a device designed to remove PM from diesel engines. CDPF forces the exhaust gas flow through the filter which traps the particles. The filter has to be cleaned regularly by regeneration processes. DOC is another after treatment device. DOC promotes chemical oxidation of HC and CO [20].

1.4.3 Emission standards for diesel engines in Europe

European emission regulations for cars and heavy-duty diesel engines, which started with Euro I and is now Euro VI (1 to 6 for passenger cars), is the emission standard for diesel engines. Emission standards became stricter. Table 1 represents CO, HC, NOx and PM emission standards for heavy-duty diesel engines and Table 2 is for passenger cars [22].

Table 1.1 EU Emission Standards for Heavy-Duty Diesel Engines, g/kWh [22]

Stage	Date	CO	HC	NOx	PM
Euro I	1992, <85 kW	4.5	1.1	8.0	0.612
	1992, >85 kW	4.5	1.1	8.0	0.36
Euro II	1996.10	4.0	1.1	7.0	0.25
	1998.10	4.0	1.1	7.0	0.15
Euro III	2000.10	2.1	0.66	5.0	0.10^a
Euro IV	2005.10	1.5	0.46	3.5	0.02
Euro V	2008.10	1.5	0.46	2.0	0.02
Euro VI	2013.01	1.5	0.13	0.40	0.01

a-PM=0.13 g/kWh for engines < 0.75 dm^3 swept volume per cylinder and a rated power speed > 3000 min^{-1}

Table 1.2 EU Emission Standards for diesel passenger cars, g/km [22]

Stage	Date	CO	HC+NOx	NOx	PM
Euro 1	1992.07	3.16	1.13	-	0.18
Euro 2, IDI	1996.01	1.0	0.7	-	0.08
Euro 2, DI	1996.01	1.0	0.9	-	0.10
Euro 3	2000.01	0.64	0.56	0.50	0.05
Euro 4	2005.01	0.50	0.30	0.25	0.025
Euro 5	2011.09	0.5	0.23	0.18	0.005
Euro 6	2014.09	0.5	0.17	0.08	0.005

1.5 European Stationary Cycle (ESC)

ESC is the European Stationary Cycle. By the Euro III emission regulation for heavy-duty diesel engines emissions, the ESC test cycle was presented with the ETC (European Transient Cycle) and the ELR (European Load Response). The ESC has 13 operating points. In this project the ESC will be used for different loads and speeds. Table 1.3 represents the ESC Test Modes. The engine has to be operated for the specified time at each point and the duration time is shown in the table [29].

Table 1.3 ESC Test Modes [29]

Mode	Engine Speed [rpm]	Load [%]	Duration [minutes]
1	Low idle	0	4
2	A	100	2
3	B	50	2
4	B	75	2
5	A	50	2
6	A	75	2
7	A	25	2
8	B	100	2
9	B	25	2
10	C	100	2
11	C	25	2
12	C	75	2
13	C	50	2

Letters represent the engine speed and numbers represent the load in %. For example, if the last operation point is C50, C is the speed and 50 is 50 % of full load. Emissions are usually measured at each operating point.

The engine speeds A, B and C is determined by using the following formulas [29]:

$$A = n_{Io} + 0.25(n_{hi} - n_{Io}) \quad (1.8)$$

$$B = n_{Io} + 0.50(n_{hi} - n_{Io}) \quad (1.9)$$

$$C = n_{Io} + 0.75(n_{hi} - n_{Io}) \quad (1.10)$$

- n_{Io} is the low speed, calculated by using 50 % of the maximum net power of the engine
- n_{hi} is the high speed, calculated by using 70 % of the maximum net power of the engine

Chapter 2

HAM - Humid Air Motor

Efficiency improvement and emission reduction can be achieved by using the evaporative cycle as a waste heat recovery technology. The steam and air mixture becomes homogeneous by using this cycle. Steam/water injection is a beneficial technology for NOx reduction and efficiency improvement. Humid Air Motor, known as HAM, is used as a waste heat recovery technology. The basic principle for the HAM working process is that hot compressed air from the compressor mixes with hot water in a humidification tower. Due to this process the mixture lowers the temperature and saturates and increases the enthalpy. Furthermore there are some main components of the HAM system known as: the humidification tower, the pressure rising pump for water, the HAM catch tank and the gas to liquid heat exchanger [27].

The HAM technology was invented in Lund University by Per Rosen 20 years ago. His concept was used for the efficiency increase of gas turbines and emission reduction in reciprocating combustion engines [24].

2.1 Early studies of HAM system

The HAM system was tested in over 100 000 hours in power plants and on board ships. HAM succeeded in emission reduction but efficiency was not deeply studied. In 2001, the HAM system was tested on an eleven liters diesel engine from Scania. The following results were obtained with variations in the load, speed and relative air humidity [24]:

- Average reduction of NOx was 51 %
- Reduction of aldehydes varied between 78 % and 100 %
- Increase in particle number concentration in the range of 46 % to 148 %
- Engine efficiency was almost unaffected

An important factor that influences NOx reduction is lower combustion temperature in the engine. NOx reduction depends on the humidity of the inlet air. Higher humidity gives higher NOx reduction. The HAM technology can probably be used in other engines. Therefore, in this thesis the investigation of the possible emission reduction and improvement of the efficiency in a heavy duty diesel engine will be studied. Hence a heavy duty diesel truck engine, which is Volvo D13 had been used for further investigations [24].

2.2 Advantages and disadvantages of the HAM technology

MAN Diesel and Turbo Company develop engines and systems for reducing the air pollution. A lot of investments have been done to make marine propulsion and power plant systems more environmental friendly. The company investigated the HAM system and found some advantages and disadvantages of using this technology. According to MAN Diesel and Turbo Company, the HAM system has the following advantages [27]:

- Low maintenance costs
- Reduction in NOx emissions up to 65 % have been achieved in demonstration tests
- Higher efficiency
- Clean combustion. Deposits in the chamber and the turbine are prevented due to the mist in the combustion chamber

And also some disadvantages, namely the following:

- A bit higher fuel consumption
- The amount of smoke in the exhaust gas is increased
- High investment costs

2.3 Working principle of HAM cycle

Figure 2.1 represents the layout of the HAM cycle simulations at the operating point A100. A100 is the operating point at 1200 rpm and 100 % load. This operating point is taken as an example in order to better understand the working principle of the HAM cycle which is described below. Figure 2.1 shows the temperature, pressure and mass flow at each component in this cycle as to have a general idea of how the HAM cycle works.

Inlet air (1) at ambient pressure and room temperature enters the compressor. After that the compressed air at 225° enters the humidity tower (2), there mass and heat transfer takes place between compressed air and water (10). Humidified air (3) has lower temperature and higher mass flow because of the humidification process in the tower. Humidification is the process of adding water vapor to the air by evaporation [25]. Humidified air mixes with the exhaust steam from a short-route EGR (9) and enters into the cylinders (4). There are two types of EGR coolers, namely the short-route and the long route. If the EGR is placed in front of the turbine it would be called a short-route EGR. Thus, if it is placed behind the turbine it would be called a long-route EGR.

Depending on the driving conditions (load and speed) and NOx reduction requirement, some part of the exhaust steam flow goes through the EGR cooler and the rest of the flow enters the turbine (6). The exhaust steam temperature decreases from 592° to 334° after the turbine for A100 and then the flow goes through the first heat exchanger (7). 90° water exits from the first heat exchanger (7). Water at 35° from the water reservoir (8) is sent to the heat exchanger (7) and takes the exhaust heat with it. The water temperature increases to 90 degrees Celsius and then this water mixes with the hot water from the EGR cooler (10). This hot water mixture is sent to the HT (2).

The exhaust steam enters the second heat exchanger (12). This heat exchanger is a condenser and the steam cools down further to 50°. From the W heat exchanger (15), cold water is sent to this

condenser. Exhaust gases go to the atmosphere and condensed water (16), which is approximately 10 % of the exhaust steam, mixes with water from the heat exchanger (15) and is fed to the water tank (8). Hot water from (12) mixes with the hot water from the HT and enters the W heat exchanger (15) for cooling [26].

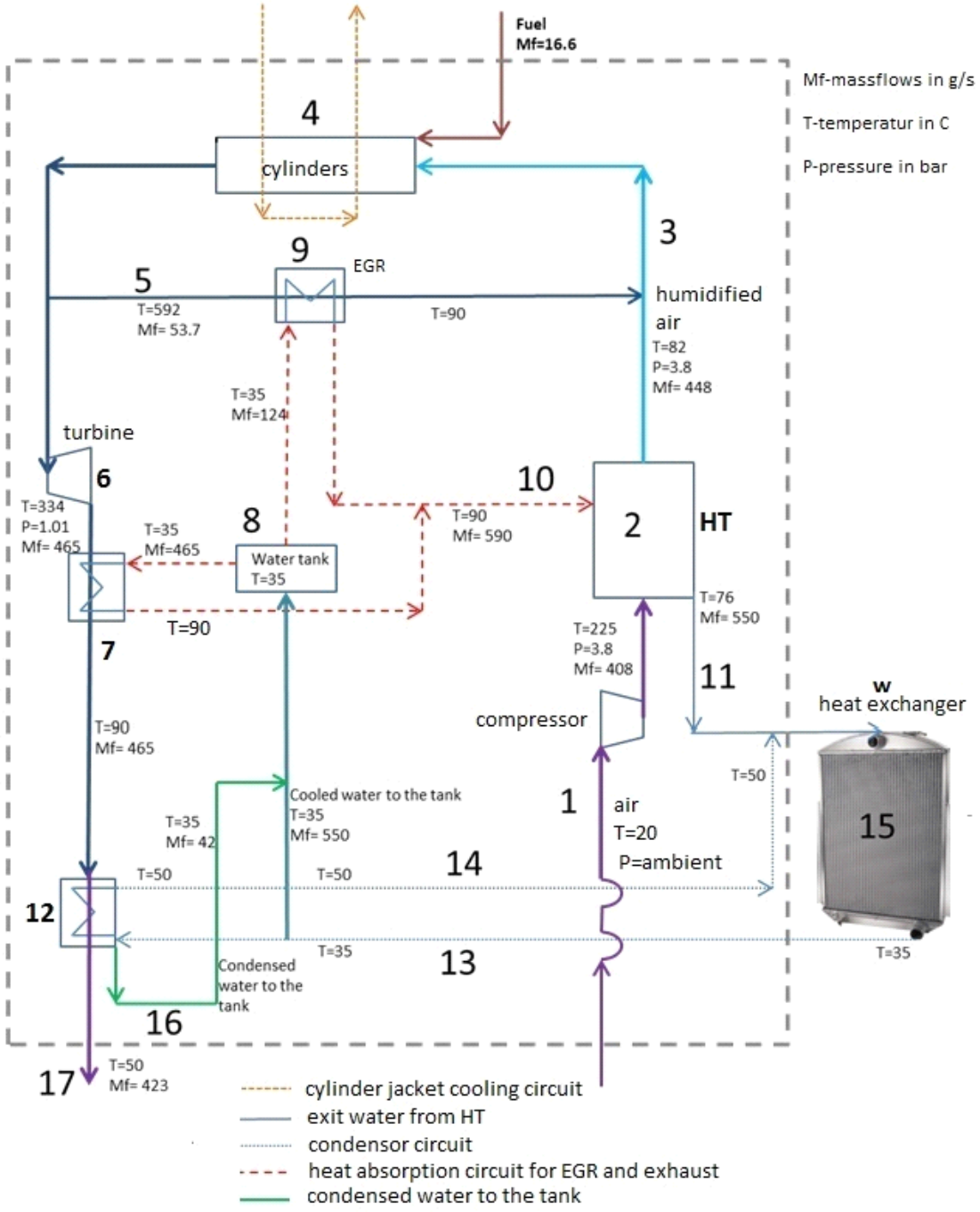

Figure 2.1 HAM engine cycle [26]

2.4 Humidification tower

For humidification of air in the HAM system, an HT (Humidification tower) is used. The HT is also called evaporator or humidifier and it is one of the main components of the HAM technology.

2.4.1 Theoretical model of the humidification tower

Theoretically, hot water that mixes with compressed air is at 90°. Considering this, the relative humidity will rise up to almost 100 %. Figure 2.2 shows an illustration of the humidification tower for the HAM cycle.

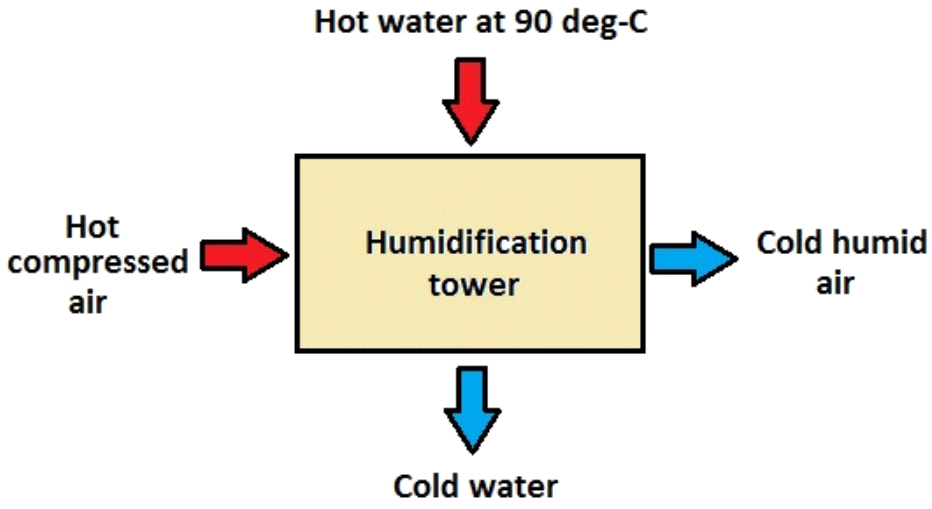

Figure 2.2 Illustration of the humidification tower for the HAM cycle

There are three important factors of vaporization in the evaporator [26]:

1. Flashing caused by higher pressure and temperature of injected water comparing with conditions prevailing in the HT

2. Vaporization through the cooling of air

3. Enthalpy change between compressed air and hot water caused by the temperature drop between the water at the inlet and outlet of the HT

The highest energy exchange between hot water and compressed air makes it possible to reach the highest evaporation ratio, i.e. evaporate a large amount of water into the dry air.

2.4.2 Thermodynamic model of the humidification tower

The thermodynamic model of the humidification tower is based on a model by Rosen and in this project MATLAB has been used when modelling the HT. Water and compressed air inlet temperatures are known. Mass flows are also known.

The following two ground assumptions have been made for the thermodynamic model of the humidification tower [26]:

- The relative humidity of the humidified air is close to 100 %
- Pinch point is the relation between the compressed air inlet temperature and the temperature of the exiting humidified water. The pinch point is the lowest temperature of the exiting water minus the temperature of the incoming compressed air. The pinch point shows in Figure 2.4, between points 2 and 3 and it has to be 3-5˚.

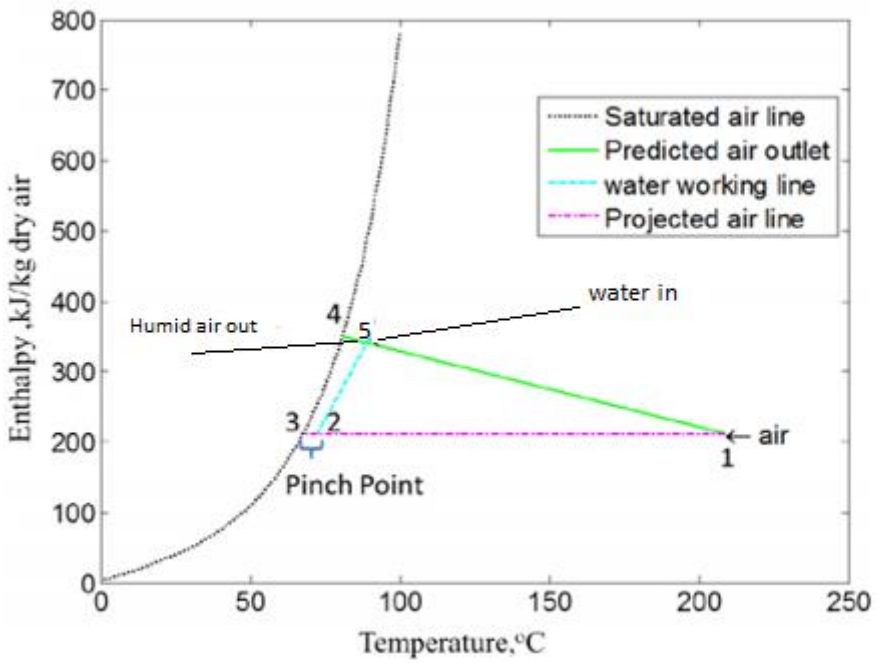

Figure 2.3 Model of the humidification tower with working lines [26]

Figure 2.3 shows how compressed air mixes with warm water. Because of the humidification process, the temperature of the compressed air and the hot water decreases. This temperature drop leads to enthalpy increase of the humid air and enthalpy decrease of hot water.

The mass flow of the humid air increases by the same amount that the mass flow of hot water decreases. Increase in mass flow leads to higher efficiency of the cycle and higher work done by the turbine. The work of the turbine is increased but without affecting the work of the compressor. Regarding that the additional work of the turbine, it could be picked up and used for extraction from the energy from the engine exhaust. For example: turbo compounding. Turbo compounding is the process of using a turbo run off exhaust gases to provide additional power to the crankshaft. By using the turbo compounding more power can be provided to the engine. In the experiments for this thesis the additional work from the turbine will not be picked up.

Chapter 3

Energy balance

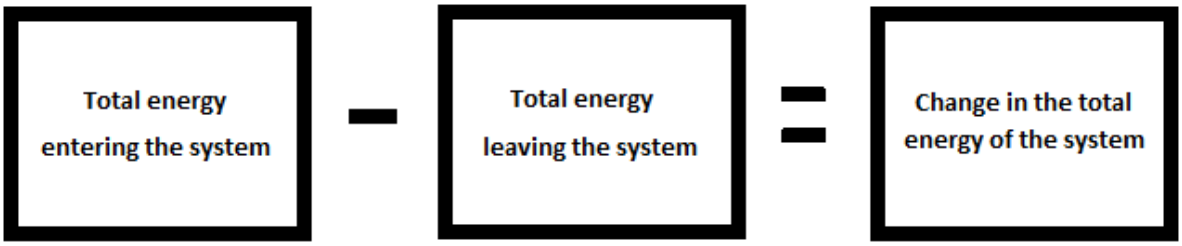

$$\underbrace{E_{in} - E_{out}}_{\text{Net energy transfer by heat, work and mass}} = \underbrace{\Delta E_{system}}_{\text{Change in internal, kinetic, potential, etc., energies}} \quad (3.1)$$

$$E_{in} - E_{out} = (Q_{in} - Q_{out}) + (W_{in} - W_{out}) + (E_{mass,in} - E_{mass,out}) = \Delta E_{system} = 0 \ (steady) \quad (3.2)$$

$$Q = \dot{Q} * \Delta t \quad (3.3)$$

Energy balance for the HAM cycle and conventional engine cycle is used for comparison of two systems at different operating points.

All calculations are based on the simulation model which was built in GT-POWER software. All equations and parameters are also taken from the simulation model. A short description of the parameters are presented below:

- Heat loss because of friction $\dot{P}_{friction}$ is calculated by the Chen-Flynn friction engine model
- Brake power ($\dot{P}_{brake}$), the useful power at the output shaft, is calculated by using the following equation. $\dot{P}_{brake} = 2\pi N\tau/60$. N is the speed in revolutions per second and τ is the torque in Nm [11]
- Heat loss in the cylinders is calculated by Woschni heat transfer model
- Loss of energy at the exhaust is calculated by the specific heat equation
- Fuel heat energy is calculated by using expression $\dot{Q}_{fuel} = \dot{m}_{fuel} * Q_{LHV}$. $\dot{m}_{fuel}$ is the fuel flow and Q_{LHV} is a lower heat value for diesel [11]
- Turbine and compressor work are taken directly from the simulation results
- Miscellaneous losses (misc) are the losses which were not taken in account but they are still present in the system. Miscellaneous losses are very small [11]

3.1 Energy balance of HAM cycle

Assumptions [25]:

1. This is a steady-flow process (no change with time at any point, delta $m_{cv} = 0$ and delta Ecv=0. CV is the control volume).
2. ke≅pe≅0, kinetic and potential energies are negligible.
3. No heat loss in the humidification tower.
4. No heat loss in the EGR cooler and in the first heat exchanger because water takes all the heat from the exhaust steam and this water is circulating in the HAM cycle.
5. Second heat exchanger has heat loss because water from this heat exchanger enters the W heat exchanger where the heat loss occurs.
6. The work done by the turbine is equal to the work required by the compressor.

$$\dot{Q}_{fuel} + \dot{W}_{comp} = \dot{W}_{turbine} + \dot{Q}_{condensation} + \dot{P}_{friktion} + \dot{P}_{brake} + \dot{Q}_{losses\ in\ cylinders} + \dot{Q}_{w\ heat\ exchanger} + \dot{Q}_{exhaust} + misc \quad (3.4)$$

$$\dot{Q}_{\ heat\ out} = \dot{Q}_{condensation} + \dot{P}_{friction} + \dot{P}_{brake} + \dot{Q}_{cylinder\ heat\ transfer} + \dot{Q}_{w\ heat\ exchanger} + \dot{Q}_{exhaust} \quad (3.5)$$

Table 3.1 Different heat parameters for the HAM cycle

Heat	is determined by using
Friction loss ($\dot{P}_{friction}$)	Chen-Flynn friction engine model
Brake power ($\dot{P}_{brake}$)	$\dot{P}_{brake} = 2\pi N\tau/60$ [11]
Heat losses ($\dot{Q}_{cylinder\ heat\ transfer}$)	Woschni heat transfer model [33]
Exhaust energy loss, $\dot{Q}_{exhaust}$	$\dot{Q}_{exhaust} = \dot{m} * Cp, avg * \Delta T$ (specific heat equation) [25]
Fuel heat energy, $\dot{Q}_{fuel}$	$\dot{Q}_{fuel} = \dot{m}_{fuel} * Q_{LHV}$ [25]
Losses in pipes and in catalyst, $misc$	$\dot{Q}_{fuel} - \dot{Q}_{\ heat\ out}$
Turbine work + compressor work	$\dot{W}_{comp} + \dot{W}_{turbine} = 0$

The HAM engine cycle was described in chapter 2. Figure 2.1 shows all the components of the system which is used for energy balance calculations. Following parts of the system have to be considered:

(7) First heat exchanger in the exhaust stream:

Given:
Exhaust mass flow from the turbine is known. In Figure 3.1 and 3.2, counter current flows and control volume on the heat exchanger can be seen. Temperature in and temperature out for water and exhaust steam are known. $\dot{m}_{exhaust}$ (exhaust steam mass flow) is also known.

Assumptions [25]:

1. This is a steady-flow process (no change with time at any point, delta $m_{cv} = 0$ and delta Ecv=0. CV is the control volume.

2. ke≅pe≅0, kinetic and potential energy are negligible.
3. Heat losses from the system are negligible Q=0.
4. No work interaction.

Mass balance: $\dot{m}_{in} = \dot{m}_{out}$ (3.6)

Energy balance: $\dot{E}_{in} - \dot{E}_{out} = \Delta E = 0\ (steady)$ (3.7)

$h = Cp * \Delta T$ (3.8)

$$\dot{Q} = \dot{m}_{exhaust} * Cp, exhaust, avg * \Delta T_{exh} = \dot{m}_{water} * Cp, water, avg * \Delta T_w \quad (3.9)$$

Now $\dot{m}_{water}$ can be calculated.

(12) Second heat exchanger in the exhaust stream:

The following are given:
- Water temperature in
- Water temperature out
- Exhaust steam flow

The latent heat of vaporization is 2257 kJ/kg at 1 bar pressure. $Q = mL$, there L is the specific latent heat, m is the mass of vapor and Q is the heat change [25]. Now the heat taken from the condensation can be found by using the equation (3.10):

$$\dot{Q}_{condensation} = (\dot{m}_{exhaust} + \dot{m}_{vapor}) * Cp, avg * \Delta T + L * \dot{m}_{vapor} \quad (3.10)$$

(9) EGR cooler:

Given:
Exhaust mass flow to the EGR cooler, temperature in and temperature out of water and exhaust steam are known.

Assumptions:
Mass balance and energy balance are the same as for the first heat exchanger [25].

$$\dot{Q} = \dot{m}_{egr} * Cp, egr, avg * \Delta T = \dot{m}_{water,egr} * Cp, water, avg * \Delta T \quad (3.11)$$

Mass flow $\dot{m}_{water,egr}$ from the water tank (8) send to the EGR cooler can be calculated now.

(15) W Heat exchanger:

This heat exchanger is used for cooling the water from the humidification tower. The amount of heat which is needed for cooling has to be calculated.

Given:

$$\text{Following are known} \begin{cases} Temperature\ water\ in \\ Temperature\ water\ out \\ Mass\ flow\ of\ water \end{cases}$$

$$\dot{Q}_{w\ heat\ exchanger} = \dot{m}_{water,HT} * Cp, water, HT, avg * \Delta T \quad (3.12)$$

(2) Humidification tower:

Total mass flow that enters the humidification tower is $\dot{m}_{water,egr} + \dot{m}_{water}$. Steps for calculation of the energy balance for the humidification tower is shown in Appendix A.

How much water mass can be recycled?

Mass of water from condensation:

1. Condensation products from exhaust steam
2. Condensation from humidified air

Total condensable mass of water can be calculated by adding $m_{exhaust\ water} + m_{ha}$. Where $m_{exhaust\ water}$ is 10 % of exhaust steam after the turbine that can be converted to water and m_{ha} is the mass of water taken from condensation of humid air.

Air can hold a certain amount of moisture and this amount depends on pressure and temperature of the air. Pressure and temperature after the second heat exchanger is known and the mass flow which does not condensate at the exhaust steam can be calculated [25].

Recyclable mass flow of water can be determined:

$$total\ mass\ flow\ recyclable = total\ condensable\ mass - mass\ flow\ escaping\ at\ the\ exhaust$$

3.2 Energy balance of conventional engine with EGR

Figure 3.1 represents the conventional engine cycle with EGR. The charger air cooler (CAC) is used for cooling down the hot compressed air after the compressor. The EGR cooler cools down the exhaust gases to be able to mix some part of the exhaust steam with fresh air before the compressor.

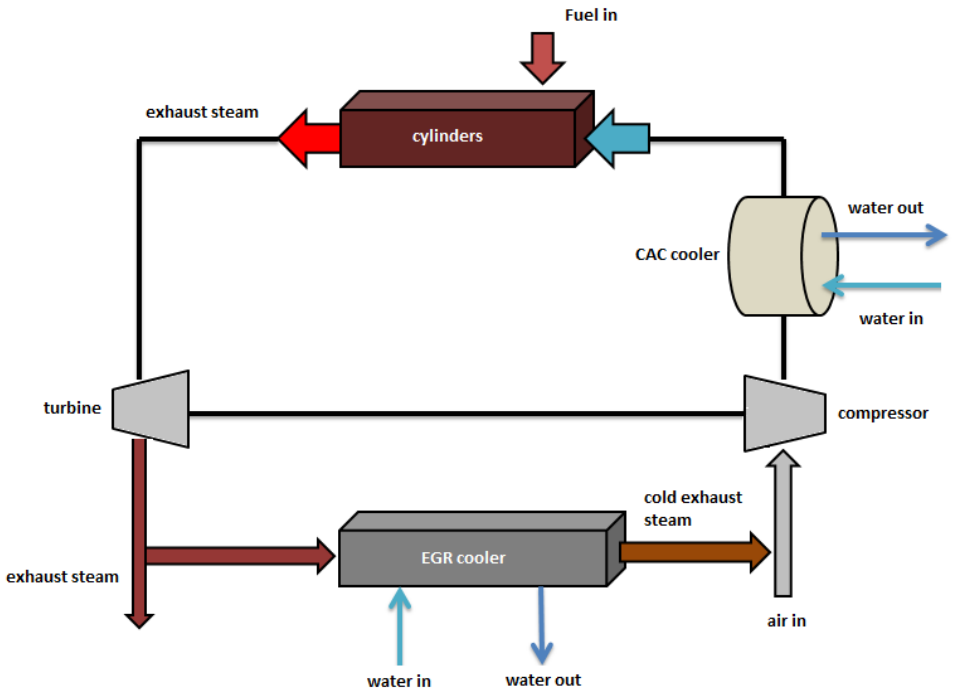

Figure 3.1 Illustration of conventional engine cycle with EGR

Assumptions [25]:

1. This is a steady-flow process (no change with time at any point, delta $m_{cv} = 0$ and delta Ecv=0. CV is the control volume).
2. ke≅pe≅0, kinetic and potential energy are negligible.

3. The work done by the turbine is equal to the work required by the compressor.

$$\dot{Q}_{fuel} + \dot{W}_{comp} = \dot{W}_{turbine} + \dot{Q}_{CAC} + \dot{P}_{friction} + \dot{P}_{brake} + \dot{Q}_{losses\ in\ cylinders} + \dot{Q}_{EGR\ cooler} + \dot{Q}_{exhaust} + misc \quad (3.13)$$

$$\dot{Q}_{heat\ out} = \dot{Q}_{CAC} + \dot{P}_{friktion} + \dot{P}_{brake} + \dot{Q}_{losses\ in\ cylinders} + \dot{Q}_{EGR\ cooler} + \dot{Q}_{exhaust} \quad (3.14)$$

Table 3.2 Different heat parameters for the conventional engine with the EGR cooler

Heat	is determined by using
Friction loss ($\dot{P}_{friction}$)	Chen-Flynn friction engine model
Brake power ($\dot{P}_{brake}$)	$\dot{P}_{brake} = 2\pi N\tau/60$ [11]
Heat losses ($\dot{Q}_{losses\ in\ cylinders}$)	Woschni heat transfer model [33]
Exhaust energy loss, $\dot{Q}_{exhaust}$	Specific heat equation ($\dot{Q} = \dot{m} * Cp, avg * \Delta T$) [25]
Fuel heat energy, $\dot{Q}_{fuel}$	$\dot{Q}_{fuel} = \dot{m}_{fuel} * Q_{LHV}$ [25]
Losses in pipes and in catalyst, $misc$	$\dot{Q}_{fuel} - \dot{Q}_{heat\ out}$
Turbine work + compressor work	$\dot{W}_{comp} + \dot{W}_{turbine} = 0$
Charge air cooler loss, $\dot{Q}_{CAC}$	Specific heat equation [25]
EGR heat loss, $\dot{Q}_{EGR\ cooler}$	Specific heat equation [25]

Table 3.2 explains how the different parameters were determined for the conventional engine cycle with EGR. The energy balance for the HAM system and for the conventional engine system with EGR will be used further in chapter 5 for comparison of the heat losses. It is also important to emphasize that in the experimental part of this thesis the conventional engine cycle will also be used without an EGR cooler. Figure 3.2 represents the conventional engine cycle without the EGR cooler.

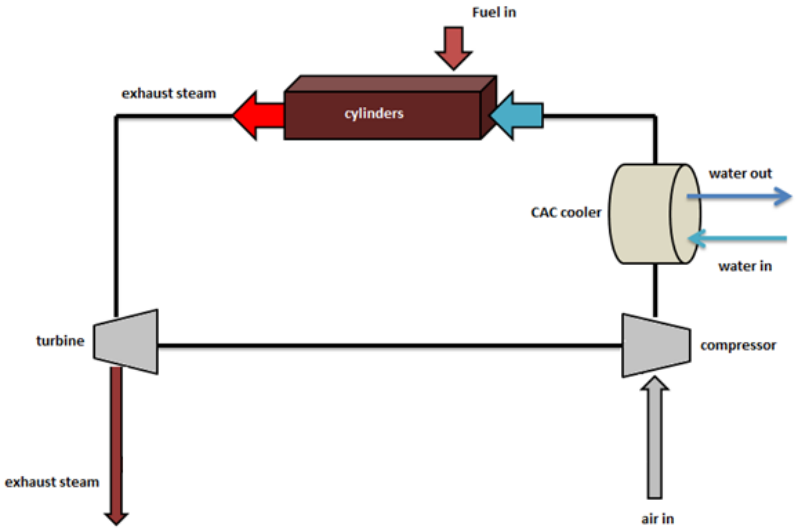

Figure 3.1 Illustration of conventional engine cycle

Chapter 4

Procedure

The objective is to study the HAM system performance in order to get a profound understanding of the advantages and disadvantages of the HAM system. The system has to be compared with the conventional diesel engine without EGR (CDC) and the conventional diesel engine with EGR (CDC-EGR). Systems have to be operated at the same conditions, namely the same operating point according to the ESC model. The measurements are performed according to the ESC test at point A25.

4.1 Engine specifications

Tests were performed with a 13 liter diesel engine with single stage turbo charging. Conventional engine setup had a short route EGR and the long route EGR was disconnected. The engine specifications are given bellow:

- 13 liter 6 cylinder 4-stroke engine
- 131 mm bore
- 158 mm stroke
- Swept Volume 13000 cm^3
- Compression ratio 16:1

4.2 Experimental HAM setup

The theoretical HAM system, namely HAM combined with EGR has already been shown in chapter 2. However, the experimental HAM setup is described in this chapter. The EGR cooler has not been used and the experimental HAM system had only one heat exchanger after the turbine. There was no condenser for condensing the water from the exhaust. The HAM setup and the working cycle of the HAM system are described below. Figure 4.2 and Figure 4.3 illustrate the HAM engine layout.

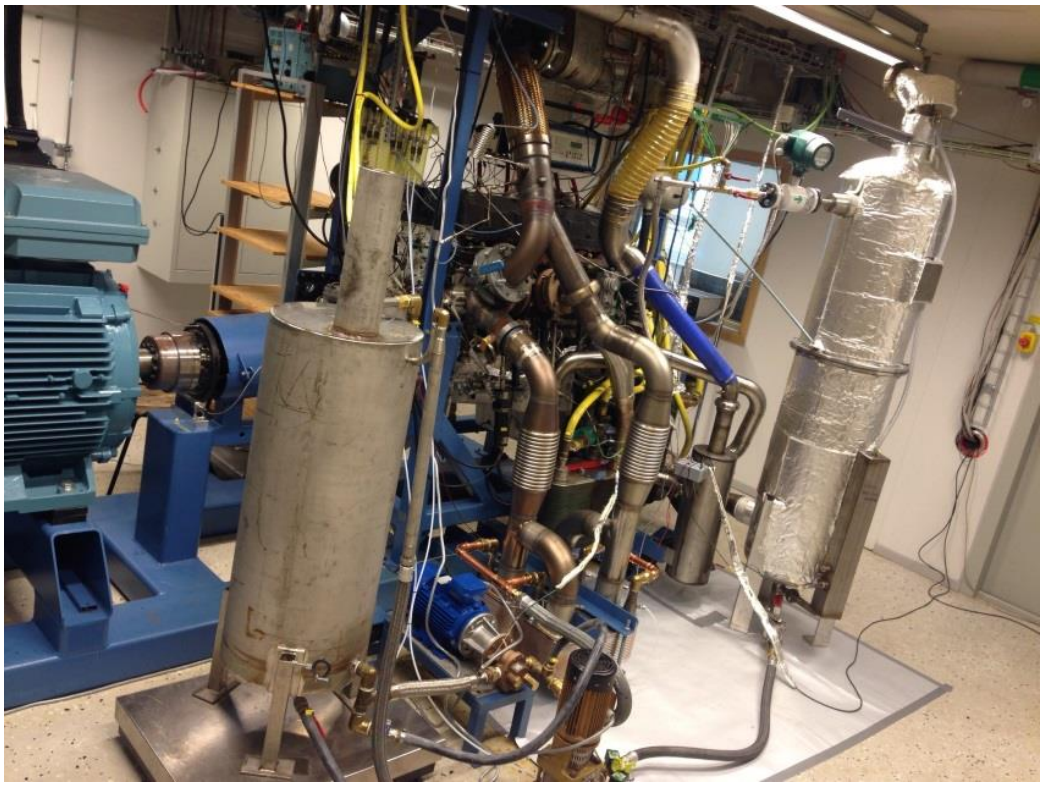

Figure 4.2 The HAM setup

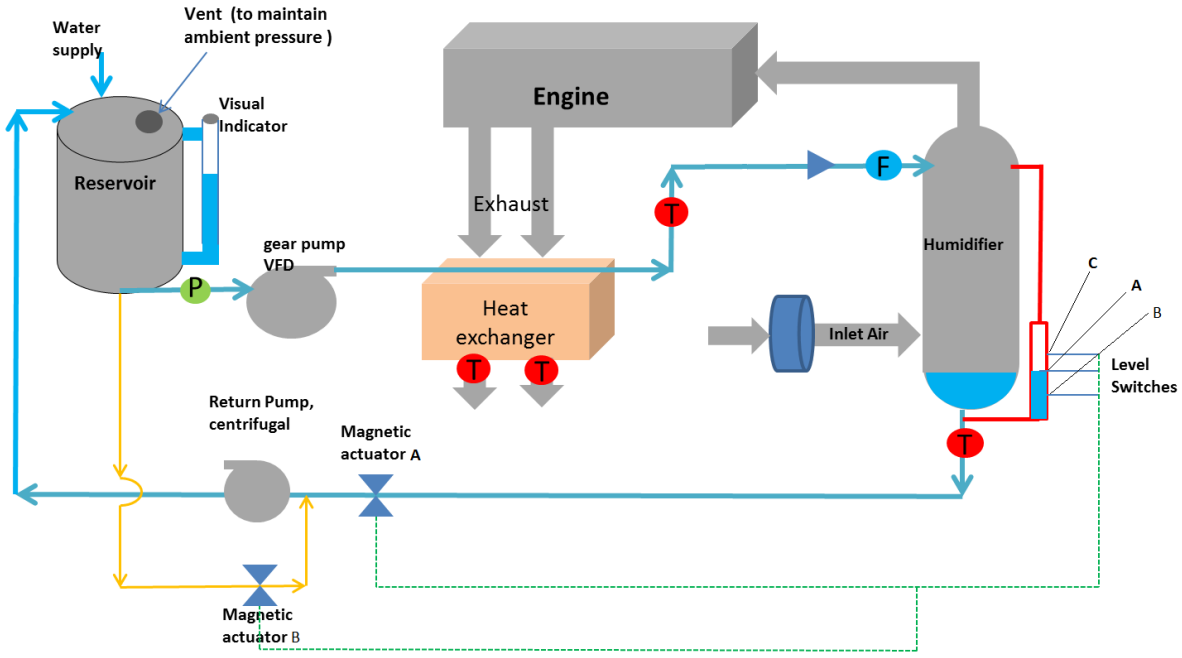

Figure 4.3 Illustration of the HAM setup

Dry air at room temperature entered the compressor and after compression, hot compressed air entered the humidifier. Hot water was fed in at 90˚. This temperature was chosen in order to avoid boiling in the heat exchangers. Mass and heat transfer between compressed air and water takes place in the humidifier. This mixing operation was countercurrent.

The easiest way of mixing water and compressed air was to have nozzles on the top of the HT and spray the hot water. Compressed air comes from the bottom of the humidifier. Some part of the hot water evaporated into the air to make the air 100 % humidified and the rest of the water flowed to the reservoir and to the heat exchanger. Just before the humidification tower, a mass flow meter was placed. The flow meter showed the mass flow of water into the humidification tower. The humidification tower had a volume of 225 liter and the maximum pressure inside could be up to 6.3 bar. Figure 4.4 shows the inside and outside of the humidification tower.

(a) outside

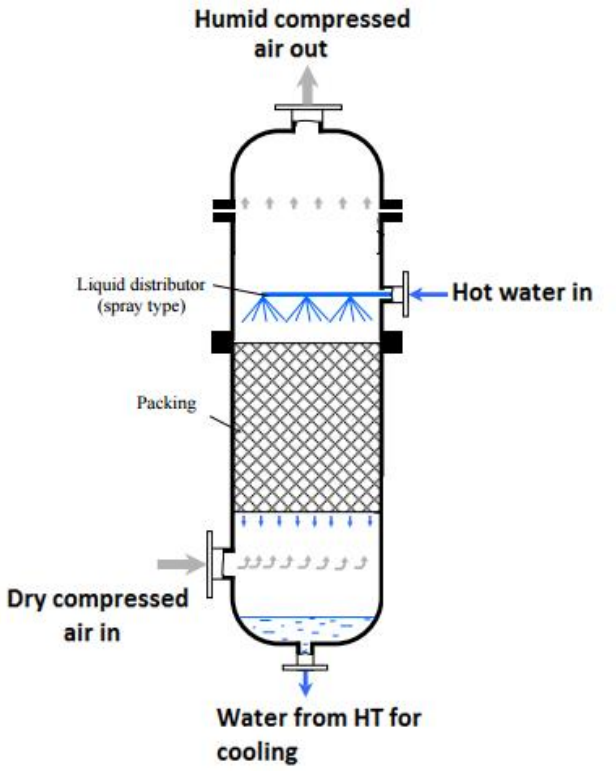

(b) inside [16]

Figure 4.4 The humidification tower

The main idea of having the structured packings inside the HT, as can be seen in the figure 4.4 (b), was to increase the surface area enhancement [16]. Those packings took up a large surface area per unit volume and had a good wetting characteristic. The nozzles and the packings can also be seen in Figure 4.5.

Figure 4.5 Packings and nozzles inside the humidification tower

Three level switches have been mounted in the steel box just beside the humidification tower. Those switches checked the water level between two set levels in the tank. The end of the steel box was welded into the bottom pipe of the humidification tower. The main reason for having the switches was to avoid the water going in to the compressor pipe.

After the humidification tower, the humidified air was fed to the engine. Hot exhaust gases entered the heat exchanger and the cold water from the water reservoir was heated up to 90˚. The water reservoir had a volume of 100 liter. The reservoir was equipped with a visual level indicator, i.e. a valve for keeping ambient pressure in the tank and water supply line from the bundling. Figure 4.6(a) represents the water reservoir.

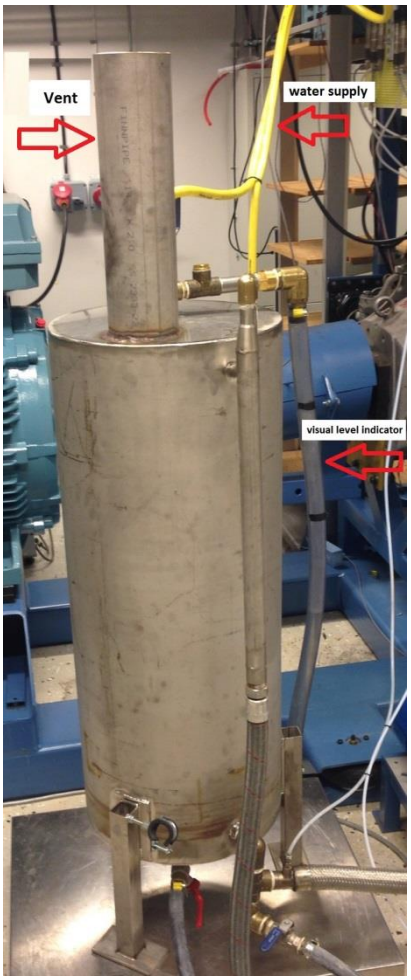

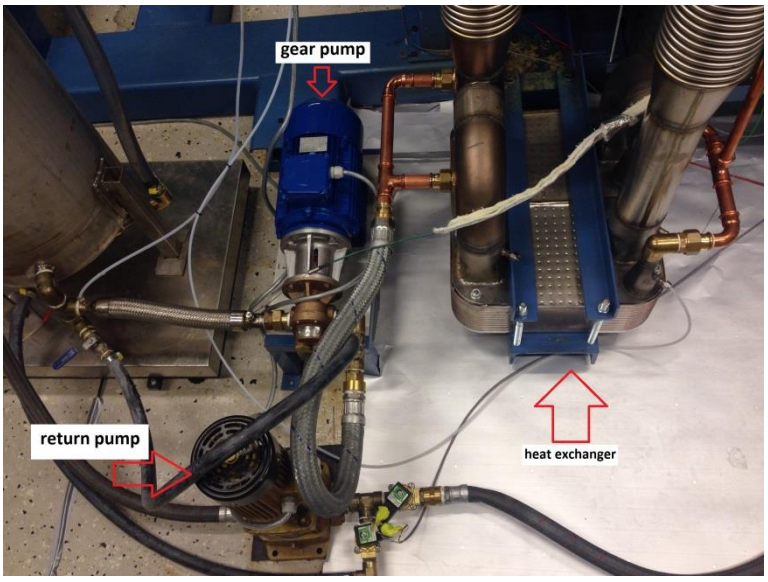

(a) the water reservoir (b) the pumps and the heat exchanger

Figure 4.6 The HAM components

The heat exchanger has two exits and at each exit the temperature sensor was placed. Letters T and P in the figure 4.3 (b) correspond to additional temperatures and pressure sensors, respectively, for the HAM setup. It was important to have additional sensors for calculation of different parameters of the system.

The gear pump was used to pump out the water from the reservoir. The speed of the pump had to be regulated in order to keep the temperature of water into the humidifier constant. A centrifugal pump was used as a return pump. The HAM system was also equipped with two magnetic actuators for maintaining the constant water lever in the humidifier.

As mentioned earlier, the HAM system was equipped with the three switches, the first one (switch C on the figure 4.3) maintained the maximum allowable water level in the tank. If for some reason switch A would not work and water would reach switch C, a signal would be directly sent to the magnetic actuators and both pumps would stop running. If water level in the humidifier would reach switch A, the gear pump would stop running, actuator A would be opened and actuator B would be closed while draining mode would take place.

After some time during the draining mode, the water would reach switch B and now the gear pump would start running. Actuator A would be closed and actuator B would be open. The return pump would still be working but just to circulate the water in and out of the reservoir. The yellow line in the figure shows that. Depending on the operating conditions and water consumption, both pumps could be running at the same time.

A weight scale was used to calculate the amount of water that has been added to the cylinders. The working principle of the scale measurement was simple. The water reservoir was placed on the weight scale and the mass of the reservoir with water was measured during the experiments. The water level in the reservoir was decreasing proportionally to the amount of water that had been placed into to the cylinders. To keep the water level in the water reservoir to a minimal, the constant water flow was fed by the water supply line. It did not affect the accuracy of the calculation of the water that had been taken by the air. The weight scale can be seen in the figure 4.6 (b).

Graphical user interface of the control program was used for reading the information from the sensors which had been placed in the engine. All data were directly displaced on the lab monitor and MATLAB was used for all calculations.

4.3 Measurement systems

A HORIBA MAXA-7500DEGR motor exhaust gas analyzer was used for the emission measurement. NOx, HC, CO and CO2 could be detected by this device. The HORIBA detection sensitivity was in a wide range. For example the sensitivity for the NOx emissions was up to 5000 ppm.

Thermo couples were used for temperature measurements of the fuel, coolant, exhaust gas and inlet air temperature. An AVL fuel scale was used for the fuel mass flow measurement.

4.4 Calculations

This section presents the formulas for calculating different parameters which was used in MALTAB.

4.4.1 Mean effective pressures and efficiencies

The mean effective pressures are shown in a Sankey diagram in Figure 4.7. The most important and relevant parts of this diagram will be explained. The Sankey diagram starts with fuel input energy (*FuelMEP*), followed by the work through the system and in the end the useful mechanical energy is presented.

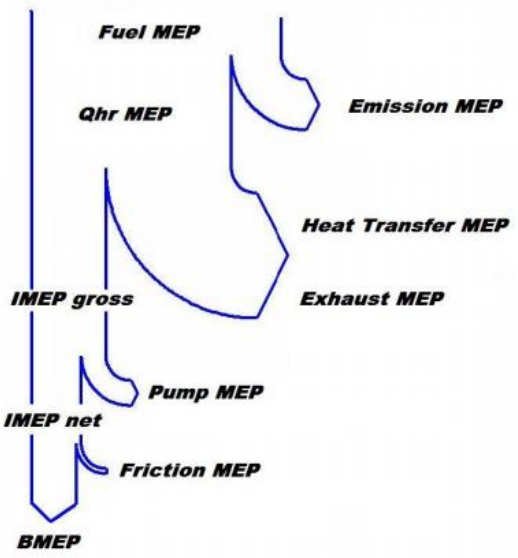

Figure 4.7 A Sankey diagram illustrating all energy transformations in pressure [bar] [33]

Fuel mean effective pressure (*FuelMEP*) is calculated as the product of fuel per cycle and the fuel's lower heating value divided by displacement volume. The engine displacement volume *Vd*, is the volume which the piston displaces during one stroke. The lower heating value for diesel fuel, which has been used for the experiments, was 43 MJ/kg. Heat mean effective pressure (*QMEP*) is the combustion process generating heat. *QMEP* shows the amount of heat released per cycle. Equations for *FuelMEP* and *QMEP* are shown below [33].

$$FuelMEP = \frac{m_f Q_{LHV}}{V_d} \tag{4.1}$$

$$QMEP = \frac{Q}{V_d} \tag{4.2}$$

$$Vd = \frac{\pi B^2}{4} Lz \tag{4.3}$$

Where B is the bore diameter, L is the stroke length, z is the number of cylinders.

IMEP is indicated mean effective pressure, designated as the work per displaced volume.

$$IMEP = \frac{W_i}{V_d} \tag{4.4}$$

IMEPg is gross indicated mean effective pressure, namely the heat that is released from the combustion is used in a thermodynamic cycle for generating work on the piston. Only the compression and expansion stroke are defined for *IMEPg.* The integration starts at BDC and ends at BDC+360 crank angle degrees [33].

$$IMEPg = \frac{1}{V_d} \int_0^{360} pdV \tag{4.5}$$

IMEPn is net indicated mean effective pressure where all four strokes are involved. The integration starts at BDC and ends at 720 crank angle degrees (two revolutions) [33].

$$IMEPn = \frac{1}{V_d}\int_0^{720} pdV \tag{4.6}$$

PMEP is the pumping losses. *PMEP* can be found as the difference between inlet and exhaust pressure. *FMEP* is the friction mean effective pressure, almost half the friction comes from piston-cylinder interaction. Brake Mean Effective Pressure (*BMEP*) is the engine output. The definition of *BMEP* is the useful energy produced by the engine per operating cycle divided by displacement volume [33].

$$BMEP = \frac{W_b}{V_d} \tag{4.7}$$

The engine total (brake) efficiency shows how much useful work that can be received from a certain amount of fuel.

$$\eta_b = \frac{BMEP}{FuelMEP} \tag{4.8}$$

The thermodynamic efficiency shows the conversion of heat to work on the piston.

$$\eta_T = \frac{IMEPg}{QMEP} \tag{4.9}$$

The gas exchange efficiency measures the ability to extract the exhaust gas and replace it with fresh air.

$$\eta_{GE} = \frac{IMEPn}{IMEPg} \tag{4.10}$$

The mechanical efficiency shows the effectiveness of the engine when transforming the energy into an output power.

$$\eta_M = \frac{BMEP}{IMEPn} \tag{4.11}$$

The last one is the volumetric efficiency that shows how efficient the gas exchange is. By using forced induction such as turbocharging, the volumetric efficiency can reach values above 100 % [33].

$$\eta_V = \frac{m_a}{\rho_{in} V d} \tag{4.12}$$

Chapter 5

Results and Discussions

The experimental results from the three different systems, namely the HAM setup, the conventional diesel engine setup (CDC) and the conventional diesel engine setup with EGR (CDC-EGR), were tested and compared at one operating point, i.e. A25. All three systems have been operated at 200 cycles and the mean value was chosen for the estimation of the results. Water temperature entering the humidifier for the HAM system was kept constant at 90˚. The inlet temperature into the cylinders was also kept constant at 60˚ for all the systems. Table 5.1 shows important parameters for the three different setups. Those parameters are helpful for understanding the achieved results in this chapter.

Table 5.1 Different parameters for the chapter 5

Different parameters	HAM	CDC-EGR	CDC
Air flow [g/s]	156	110	163
Air flow [g/s] at VGT=50 and SOI=0	156	112	162
Lambda [-]	2.4	1.8	2.4
P inlet [bar]	1.6	1.5	1.4
CA50 [CAD ATDC]	9.6	7	11
CA50 [CAD ATDC] at VGT=50 and SOI=0	9.6	10.6	9
T inlet [˚]	59.9	60.3	60.5
Bsfc [g/kWh]	222	219	224

5.1 Choosing the best operating condition

A25 was chosen as a reference point for all the systems. According to the ESC the A25 operating point had the speed 1200 rpm and torque 600 Nm (varied between 599 and 610 Nm because of the discrepancies in the injector control).

Each system had the best operating condition among the different operating conditions. The different operating conditions have been achieved by changing two parameters of the systems, namely by changing the start of injection (SOI) and the variable-geometry turbocharger (VGT) position. SOI was varied between -6 and up to 2 CAD. The VGT position was varied between 30 and 70 %. Variations in the parameters are shown in table 5.2. The HAM system, the CDC-EGR system and the CDC setup have been running at 25 different operating conditions at one operating point A25.

Table 5.2 Variations in the parameters

SOI:	2	0	-2	-4	-6
VGT:	70	60	50	40	30

The main purpose with the HAM system was to reduce NOx emissions and specific fuel consumption. Trade-off between NOX and *bsfc* can be seen in Figure 5.1. The blue line shows the NOx emissions in *g/kWh* and the green line shows the specific fuel consumption in *g/kWh*. The best operating point according to the figure was at SOI 0 CAD and VGT 50 %.

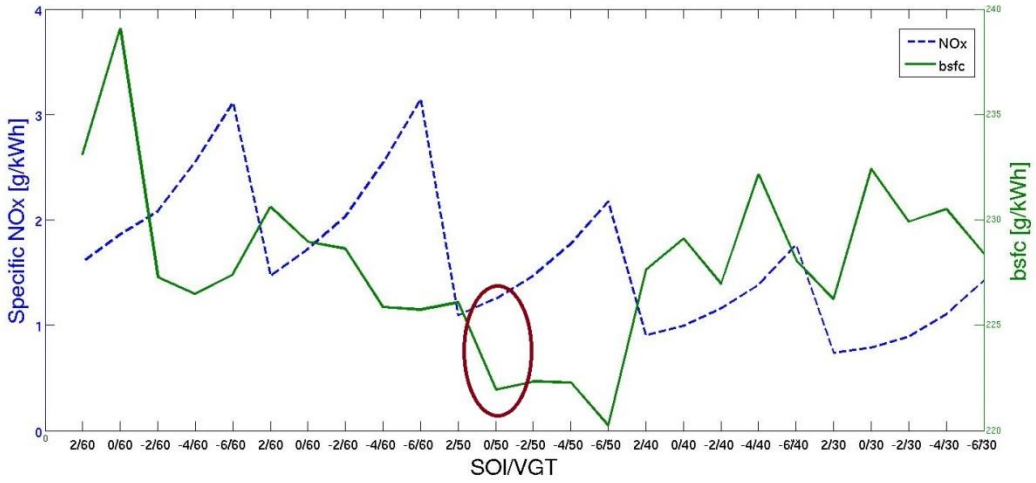

Figure 5.1 Trade-off between NOx and *bsfc* for the HAM system at A25

The same procedure has been done for the conventional engine operation and the conventional engine operation with EGR. 37% EGR was used for the operation with EGR. This value was taken from the simulation result (which originally was taken from engine experiments). Figure 5.2 and 5.3 shows trade-off between NOx and *bsfc* for the CDC-EGR and the CDC systems at A25.

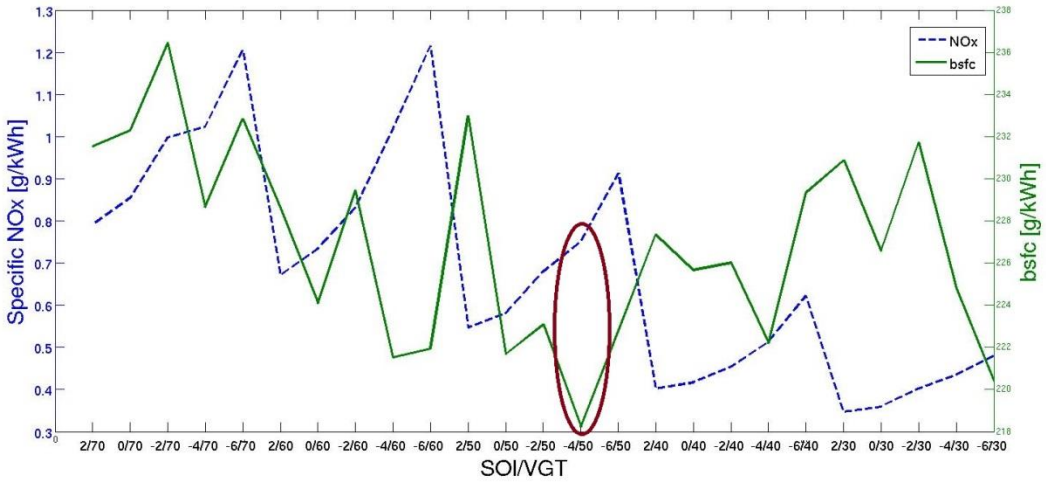

Figure 5.2 Trade-off between NOx and *bsfc* for the CDC-EGR system at A25

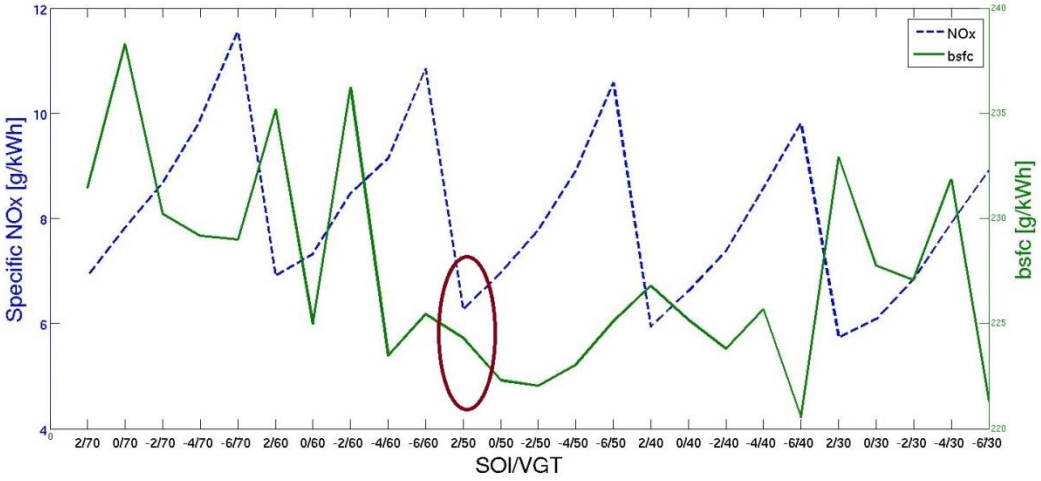

Figure 5.3 Trade-off between NOx and *bsfc* for the CDC system at A25

The main reason to why it was a priority to choose the lowest *bsfc* was because the NOx emissions could be reduced by using the catalysts. In the figures above, the NOx values were little bit higher than the values of *bsfc*. However, no catalysts have been used for emission reduction during the experiments.

The following parameters have proven to be the best:

- The HAM setup with VGT=50 and SOI=0
- The CDC-EGR setup with VGT=50 and SOI=-4
- The CDC setup with VGT=40 and SOI=2

5.2 Mean effective pressures

To be able to decide which system is more beneficial in terms of NOx and *bsfc* reduction, mean effective pressures of different parameters are compared.

5.2.1 IMEPg

Figure 5.8 shows the difference in a mean gross effective pressure for the systems. The *PMEP* is a difference between *IMEPg* and *IMEPn.* For understanding the figure 5.4, the *PMEP* values and the *IMEPn* values have to be investigated.

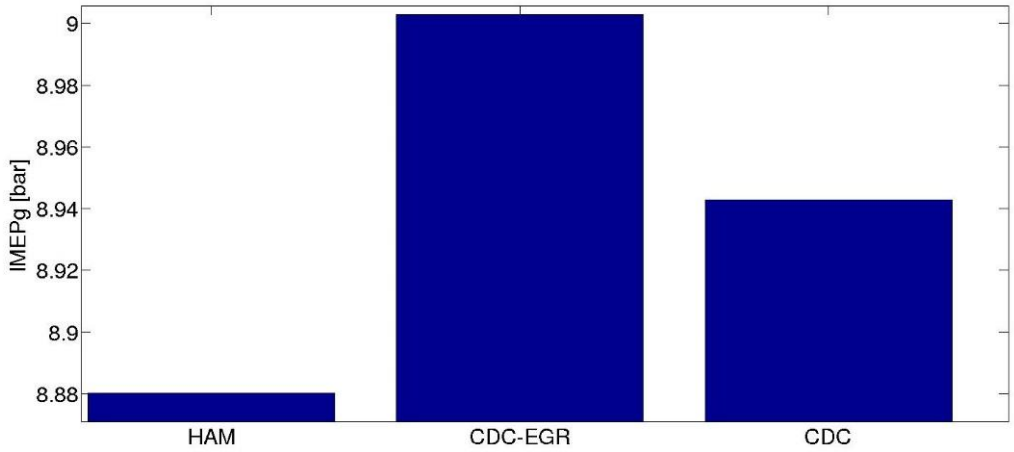

Figure 5.4 *IMEPg* values for the different systems

5.2.2 PMEP

PMEP is one of the important losses. Figure 5.5 illustrates pressure as a function of volume for the systems. As it can be seen in this figure, the highest pressure loss was in the CDC system and the lowest pressure loss was in the HAM setup. The distance between points A and B in the figure corresponding to the pressure drop. Bigger distance gives higher losses.

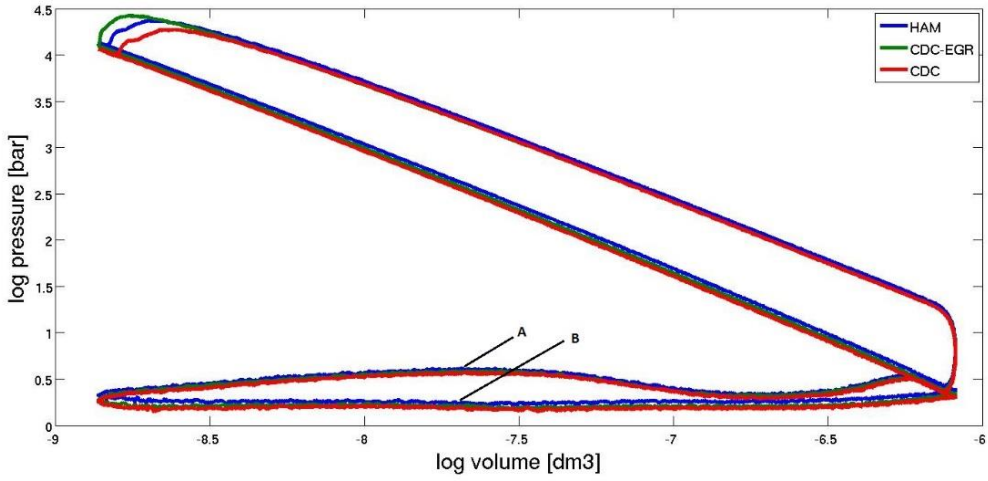

Figure 5.5 Pressure as a function of volume for the systems

The CDC and the CDC-EGR systems had almost the same *PMEP* values. In order to explain why the HAM system had the lowest pressure drop, the inlet and the exhaust pressures have to be compared. The exhaust pressures were the same for the three systems. HAM inlet pressure was around 1.6 bar and the CDC setup had around 1.4 bar. Those values can be seen in the table 5.1. Generally, a higher inlet pressure gives lower pressure loss. By adding the water into the cylinders, it gives additional enthalpy to the turbine because of the increased mass flow. In turn it gives also lower pumping losses [11]. The explanation of why CDC-EGR had lower pumping losses then the CDC system was the same. EGR gave more enthalpy to the turbine. The *PMEP* values are shown in Figure 5.6.

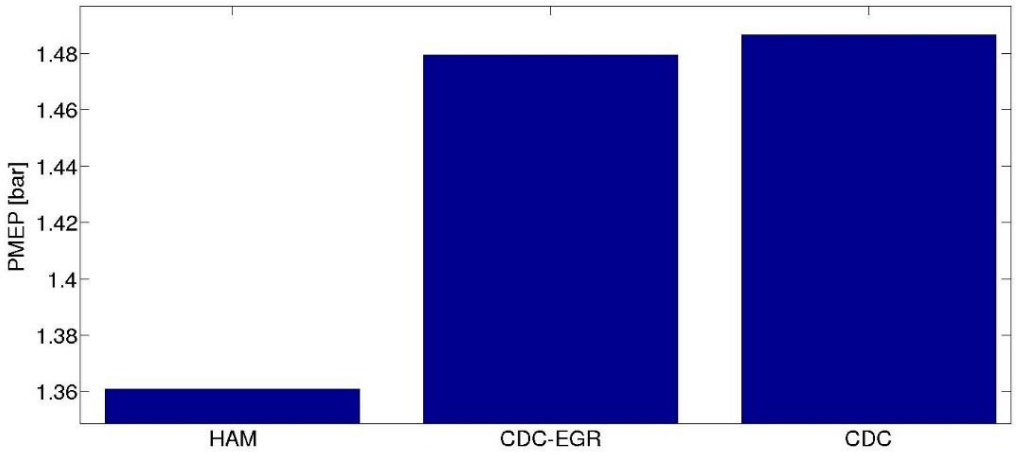

Figure 5.6 *PMEP* values for the different systems

5.2.3 IMEPn

The work on the piston, *IMEPn*, depends on the *IMEPg* and the *PMEP* values. As it was already mentioned before, *PMEP* had the lowest value for the HAM system and the highest value for the CDC.

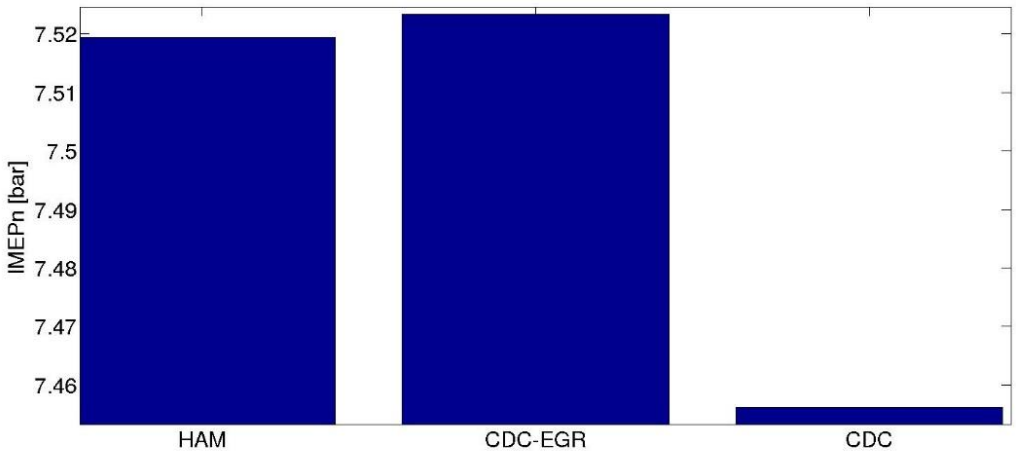

Figure 5.7 *IMEPn* values for the different systems

5.2.4 FMEP

Friction in the engine was the same for all systems because the same engine was used for all the three systems. Figure 5.8 shows the *FMEP* values.

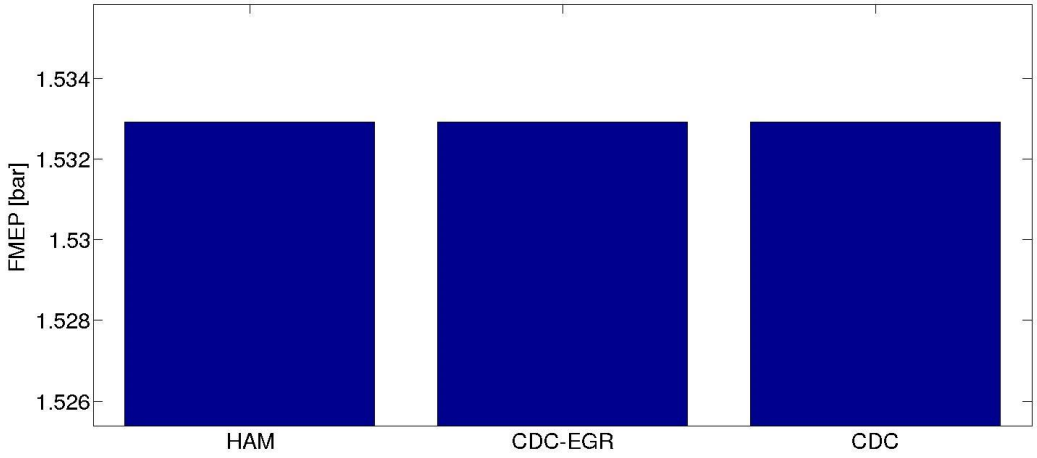

Figure 5.8 *FMEP* values for the different systems

5.2.5 BMEP

Figure 5.9 represents the *BMEP* values for the systems. As it can be seen in the figure, *BMEP* was almost the same. Measured torque value for the best HAM operating point was around 609 Nm and for the conventional engine setup it was around 610 Nm. The main idea was to keep the same torque value for all the setups in order to make correct comparisons of the systems. Varying the VGT position and SOI gave a bit different torque values. The compensation with injection timing was rudimentary and that resulted in torque discrepancies. *BMEP* had the same trend as was expected.

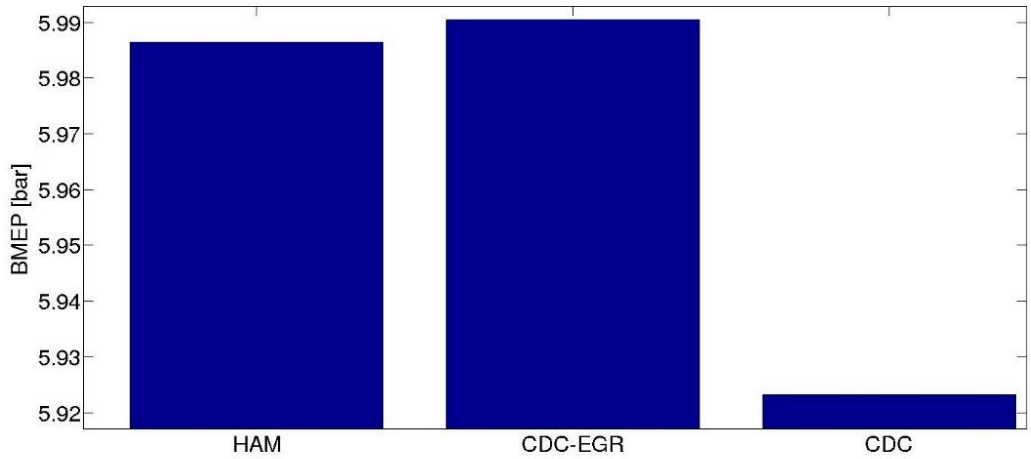

Figure 5.9 *BMEP* values for the different setups

5.3 Efficiencies

The brake efficiency shows the effectiveness of the total system. The brake, mechanical, gas exchange and the thermodynamic efficiency values for the HAM, CDC-EGR and the CDC setups are given in Figure 5.10. The HAM system had 0.7 % lower engine efficiency than CDC-EGR and 0.4 % higher than the CDC system.

For deeper understanding as to why HAM had the lower total efficiency, four different efficiencies dealing with thermodynamics, gas exchange, friction and combustion have to be investigated. Table 5.3 shows the values of the different efficiencies.

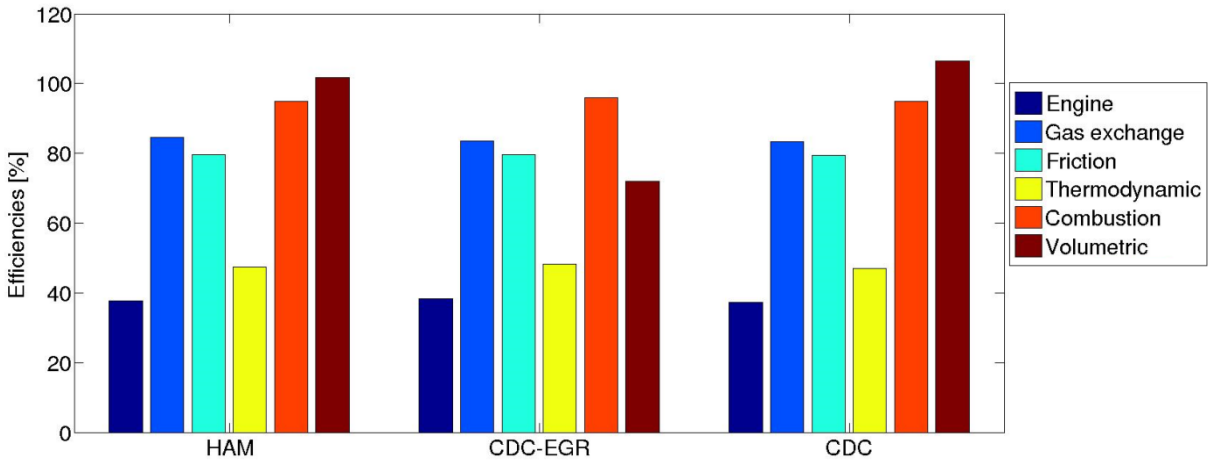

Figure 5.10 Engine, gas exchange, mechanical, thermodynamic, combustion and volumetric efficiencies for the HAM, CDC-EGR and CDC setups

Table 5.3 The efficiencies in % for the HAM, CDC-EGR and CDC systems

Systems	Engine	Gas exchange	Friction	Thermodynamic	Combustion	Volumetric
HAM	37.7	96.5	79.6	51.7	95	102
CDC-EGR	38.4	96.3	79.6	52	96	72
CDC	37.3	96.2	79.5	53.4	95	107

Scavenging needs some work to be done. The gas exchange efficiency depends on PMEP, temperature of inlet gas and boost. It was already discussed that HAM had the lowest pumping work. It clearly explains that the gas exchange efficiency for the HAM setup would be highest. This was also confirmed by figure 5.10 above. The gas exchange efficiency for HAM was 0.2 % higher than for CDC-EGR and 0.3 % higher than for the CDC system.

The mechanical efficiency of the systems was influenced by friction (FMEP) and load. The engine has been tested at the constant load [11]. The FMEP values were the same for the different setups and that in turn determined the mechanical efficiency of the engine.

The thermodynamic efficiency is the conversion of the heat to work on the piston. The thermodynamic efficiency was highest for the CDC-EGR system. The main reason for that was due to *IMEPg* and heat transfer losses to the walls of the combustion chambers. *IMEPg* was highest for CDC-EGR. The heat transfer losses to the wall will be seen in section 5.4.

The HAM system had 1.7 % lower thermodynamic efficiency than CDC and 0.3 % lower than the CDC-EGR setup.

The combustion efficiency was almost the same for the systems. The values of the combustion efficiency seem to be a little bit low. It can be explained by the cylinder to cylinder variations which affected the total heat release rate. The average value of the Q_{in} values for the six cylinders was used in the calculations.

Last but not least, is the volumetric efficiency. It was highest for the CDC setup and lowest for CDC-EGR. To investigate why this occurred, lambda values should be seen. The CDC system had the lambda around 2.5. CDC-EGR had a rich combustion with lower access to the air. The lambda value was 1.7.

Now have a look at the mass flow of air for the systems. The air mass flow for the systems can be seen below:

- 163 g/s for the CDC system
- 156 g/s for the HAM system
- 110 g/s for the CDC-EGR system

The inlet temperature was the same for all three systems. In turn it means that the air density was also the same. The HAM system had lower air flow compared to CDC, due to additional mass of water. The CDC-EGR setup had even less air flow because of 37 % EGR. HAM had higher volumetric efficiency than the CDC-EGR system because the turbine had more enthalpy, due to increased mass flow of humid air in to the cylinders. The efficiency was increased by 30 % compared with CDC-EGR.

5.4 Heat losses

Another significant parameter which describes the performance of the systems is heat losses. This section presents energy losses for the HAM, CDC-EGR and the CDC systems. The following losses were taken into account: friction losses, pumping losses, losses at the exhaust, heat transfer losses, losses in the cooler, combustion losses and miscellaneous losses. Figure 5.11 shows a comparison between the HAM, CDC-EGR and the CDC systems.

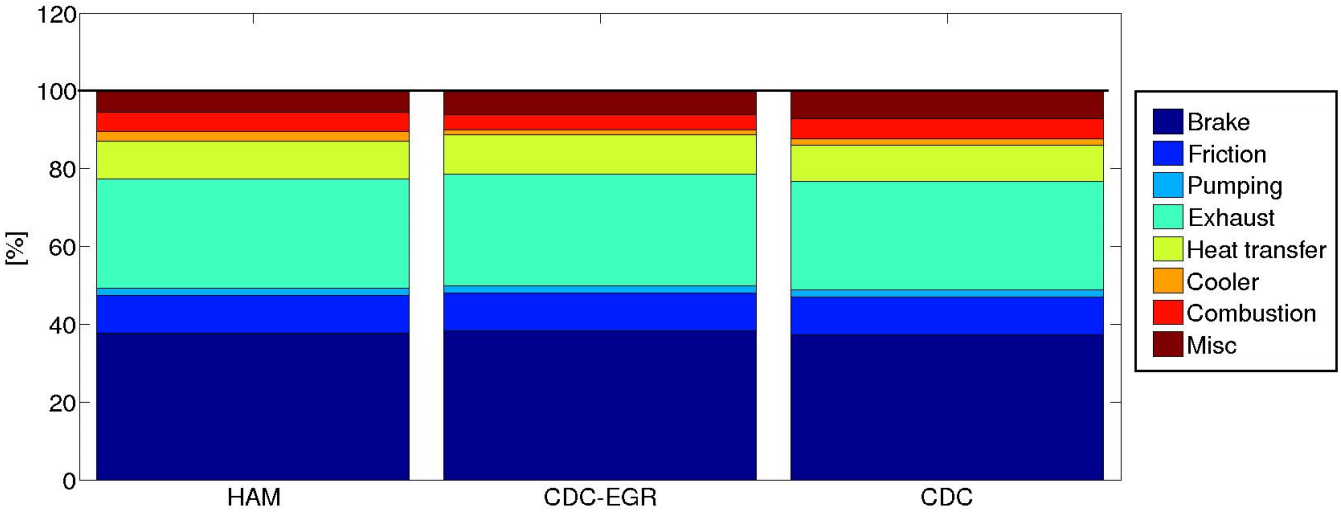

Figure 5.11 Comparison of loss terms in % of fuel energy for the HAM, CDC-EGR and the CDC systems

The losses from each part of the systems for the A25 operating point are represented in table 5.4. Figure 5.12 represents the definition of location for the energy sources represented in table 5.4. For clarification of figure 5.12, the following aspects must be brought forth: the friction losses are in the crankshaft (1), the pumping losses included the losses in the compressor and the turbine (2), the losses at the exhaust (3), the heat transfer losses are in-cylinder heat transfer losses (4), the combustion losses (5) and the losses in the cooler (6). The miscellaneous losses were described in the chapter 3.

Table 5.4 Heat losses and power in kW and % of fuel energy for different systems

HAM			**CDC-EGR**			**CDC**		
Fuel Power	**[kW]** 203	**[%]**	*Fuel Power*	**[kW]** 199	**[%]**	*Fuel Power*	**[kW]** 203	**[%]**
Brake Power	76	38	*Brake Power*	77	38	*Brake Power*	76	37
Total losses	**127**	**-**	***Total losses***	**122**	**-**	***Total losses***	**127**	-
Friction	20	10	*Friction*	20	10	*Friction*	20	10
Pumping	4	2	*Pumping*	4	2	*Pumping*	4	2
Exhaust	57	28	*Exhaust*	59	29	*Exhaust*	58	28
Heat Transfer	20	10	*Heat Transfer*	20	10	*Heat Transfer*	19	10
Cooler	5	3	*Cooler*	3	1	*Cooler*	3	2
Misc	18	6	*Misc*	20	6	*Misc*	22	8
Combustion	-	5	*Combustion*	-	4	*Combustion*	-	5

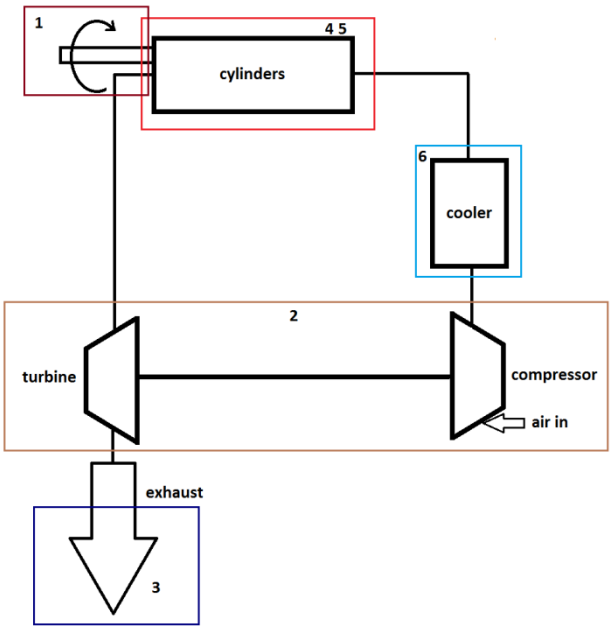

Figure 5.12 Definition of location for the energy sources presented in Table 5.4

Since the HAM system is a waste heat recovery technology, some part of the exhaust energy was recuperated in the cycle. The total heat loss at the exhaust for the HAM system was 57 kW. Some part of that heat was used for warming up the water from the water reservoir. 67 % (38kW) of the total exhaust loss was used for warming up the water and in this case it could not count as a loss. In figure 5.11 the total heat at the exhaust was presented, namely 57 kW (38kW was used for warming up the water and 19 kW was the actual loss at the exhaust). The heat energy to cool down the circulating water inside the humidification tower was included in the cooler heat losses. The EGR cooler heat loss was included in the exhaust energy losses as it was a long route EGR.

5.4.1 In-cylinder heat transfer losses

For deeper understanding of in-cylinder heat transfer losses, a heat release rate (HRR) and a cumulative heat release will be investigated. Figure 5.13 displays the peak rates of heat release for different systems. In general, retarding SOI makes the peak values decrease because of decreased bulk temperature. The HRR is also influenced by the inlet temperature but in this experiment the inlet temperatures were the same for all systems. It can be seen in the figure that the HAM system had the highest peak rate and this behavior could be explained by the late SOI.

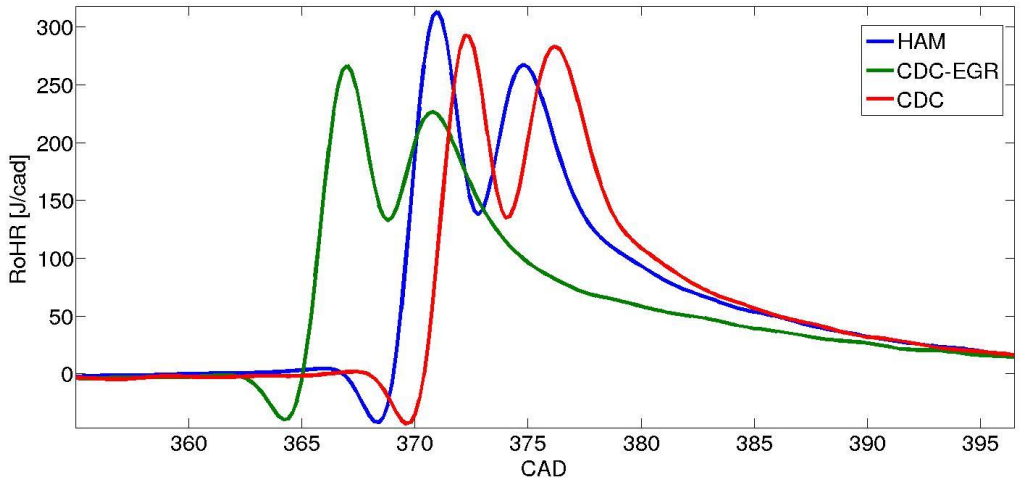

Figure 5.13 Heat Release Rate for the different systems

Another parameter which directly affects the in-cylinder peak temperatures and peak rates is CA50. CA50 (combustion phasing) is the crank angle ATDC at which 50 % of total heat release occurs. Namely 50 % of fuel mass is burned [34]. Figure 5.14 illustrates CA50 as a function of in-cylinder peak temperature at different SOI for the HAM system. It clearly shows that a lager value of the CA50 value gives lower peak temperature. Back to Figure 5.13, CA50 for CDC was 11 CAD ATDC and for the HAM system this value was around 9.6 CAD ATDC. It explains why the peak rate of the heat release for the HAM setup was higher.

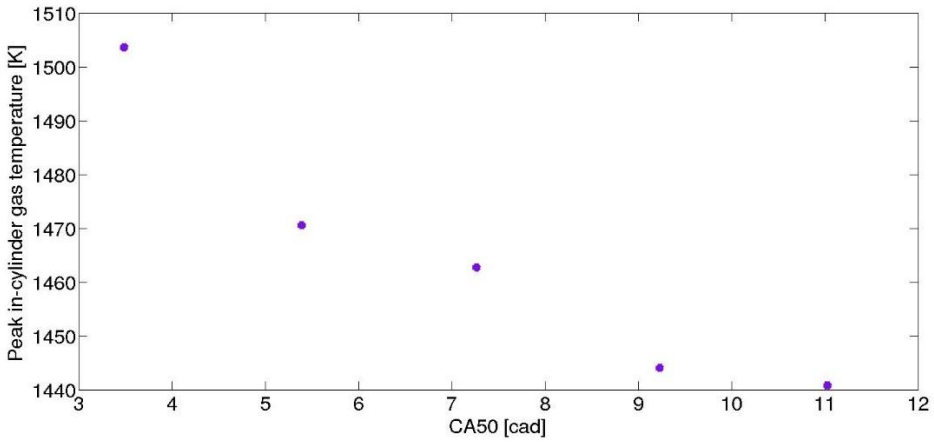

Figure 5.14 CA50 as a function of in-cylinder peak temperature for the HAM system

Accumulated heat release rate is shown in Figure 5.15. Because of different operating parameters of the engine setups, the HAM system had the highest heat losses. It can be seen in the figure where it is clearly visible that SOI was different. The region named by letter A shows that.

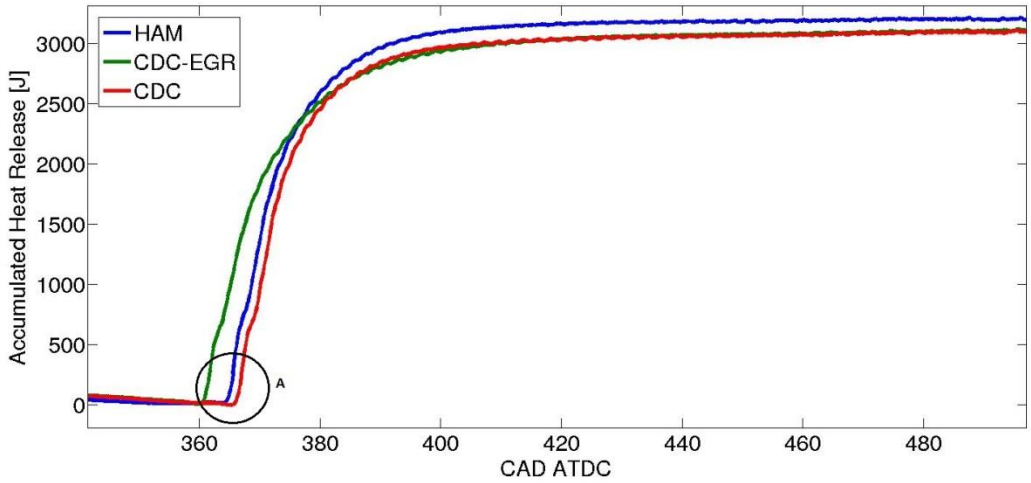

Figure 5.15 Accumulated heat release rate for the different systems

Heat losses to the combustion chamber walls are a part of the total in-cylinder heat losses. Woschni's Heat transfer model was used for the calculation of the heat losses to the combustion chamber walls.

The CDC-EGR setup had higher heat losses to the walls. Losses for the HAM setup were around 19 kW and that was 2.4 % lower compared with CDC-EGR. This is shown in Figure 5.16. The heat losses to the walls for the CDC-EGR system accounted for 20 kW. In the HAM system, the water vapor absorbed some amount of heat in the cylinders and that helps reduce the peak temperature which in turn helps us in reducing the heat transfer. CDC had lowest losses to the walls because of lowest peak pressure in the cylinders in comparison to CDC-EGR. The in-cylinder pressure and temperature have a direct affect on the heat transfer. In this case CDC had the lowest in-cylinder pressure and that's why the heat transfer was the lowest in the CDC system.

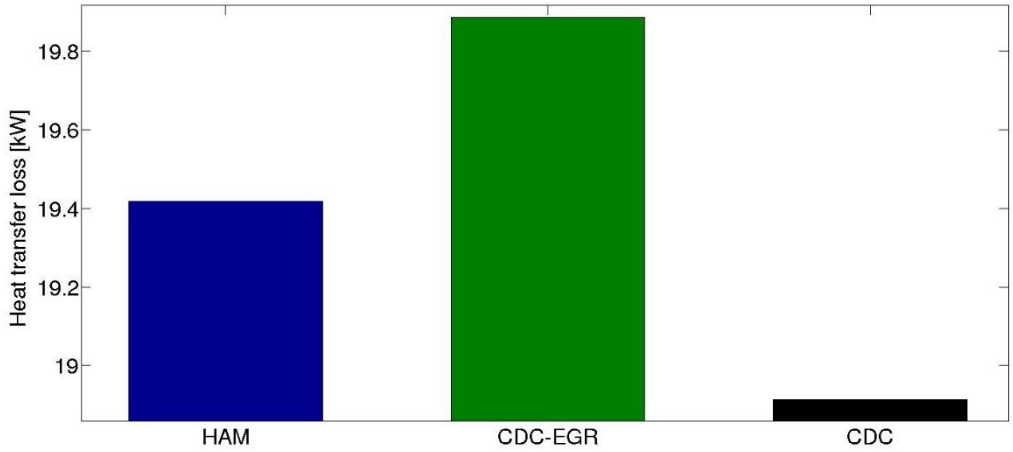

Figure 5.16 Heat losses to the combustion chamber walls for the different systems

5.5 Emissions

5.5.1 NOx

One of the most important features with the HAM system concept is to reduce NOx emissions. Figure 5.17 represents the NOx emissions for the three setups. It was expected that CDC would have the highest values of NOx. The main thing was to see the difference between HAM and CDC-EGR. The HAM setup had 1.3 g/kWh NOx emissions and this value for CDC-EGR was around 0.7 g/kWh. It means that HAM had 1.6 times higher NOx emission than the CDC-EGR system and 5 times less than CDC.

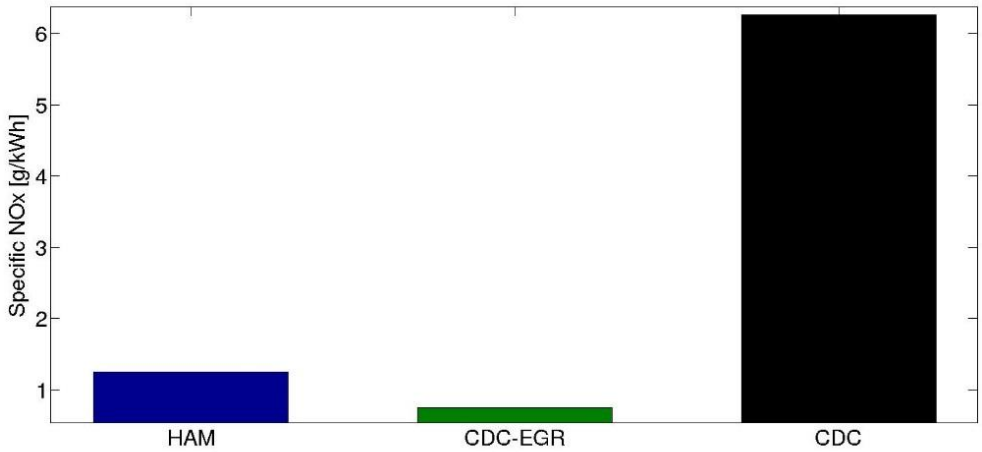

Figure 5.17 Specific NOx emissions for the different systems

To understand why HAM had the higher value of NOx emissions, Figure 5.18 is very helpful. Generally, high peak in-cylinder temperature directly increases the NOx formation. Of course it is important to remember that the local temperate is lower than the in-cylinder peak temperature and most of the NOx emission production occurs in the zones with high local temperature.

This explains why CDC had the highest NOx emissions. Figure 5.18 shows that CDC-EGR had highest peak temperature than HAM but still the NOx emissions were lower. Another significant parameter which affects the NOx formation was the oxygen concentration available for the production of NOx. As it was already mentioned before, NOx forms with high access to the oxygen. Air flow for the HAM setup was 156 g/s and for CDC it was around 110 g/s. It explains why the HAM system had higher emissions of NOx compared with CDC-EGR.

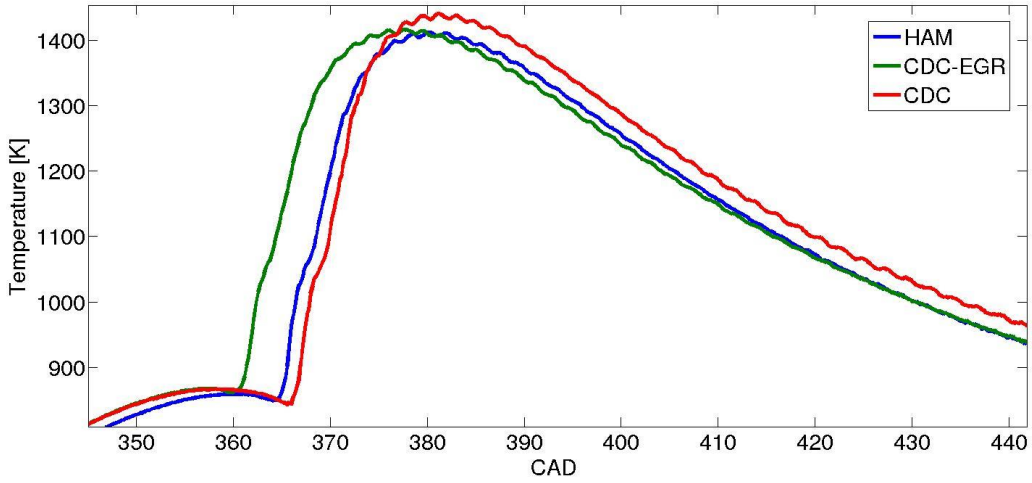

Figure 5.18 In-cylinder temperatures for the different systems

In figure 5.18 the systems were compared at the different operating conditions, namely at the different SOI and VGT. It would be interesting to see how the HAM system would behave if the operation parameters would be the same. The three setups compared at the same SOI and VGT can be seen in Figure 5.19. SOI and VGT for the HAM setup were taken as a reference. Keep in mind that SOI was 0 CAD and the VGT position was 50 %.

The figure clearly displays that CDC-EGR had the lower peak temperature than the HAM system. This occurred perhaps because of the lower amount of water fed to the system compared to the amount of EGR. This water amount was not enough to absorb the heat in charge to reduce the peak temperature as much as EGR could. The water added to the system is directly dependent on the speed and the load at which the system is operated.

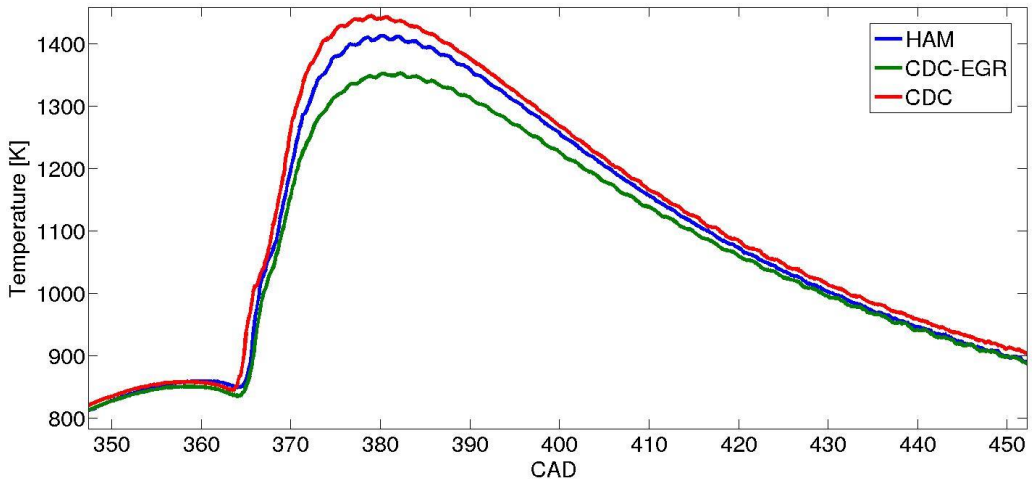

Figure 5.19 In-cylinder temperatures at the same operating conditions

The peak pressure as a function of crank angle is illustrated in Figure 5.20. The CDC system had the lowest peak in-cylinder pressure because of the lowest inlet pressure to the manifold. The inlet pressure for CDC was 1.4 bar at the best operating point and for HAM that pressure was around 1.6 bar. CDC-EGR had a bit lower inlet pressure, 1.50 bar. As was mentioned before, all the systems were operated at different operating parameters.

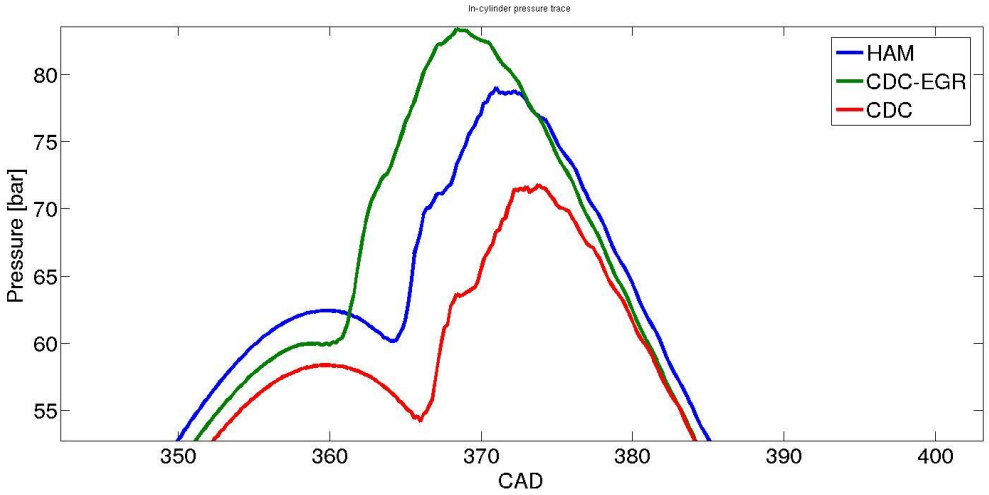

Figure 5.20 In-cylinder peak pressures as a function of crank angle for the different systems

Now figure 5.21 shows the pressure as a function of crank angle at the same SOI and the VGT position (SOI=0, VGT=50). The lowest inlet pressure was in the CDC setup but still the peak pressure was higher than in the CDC-EGR case. This could be explained by the fact that CA50 for CDC-EGR was higher and it means that the peak in-cylinder temperature was lower. In turn the peak pressure showed that kind of trend.

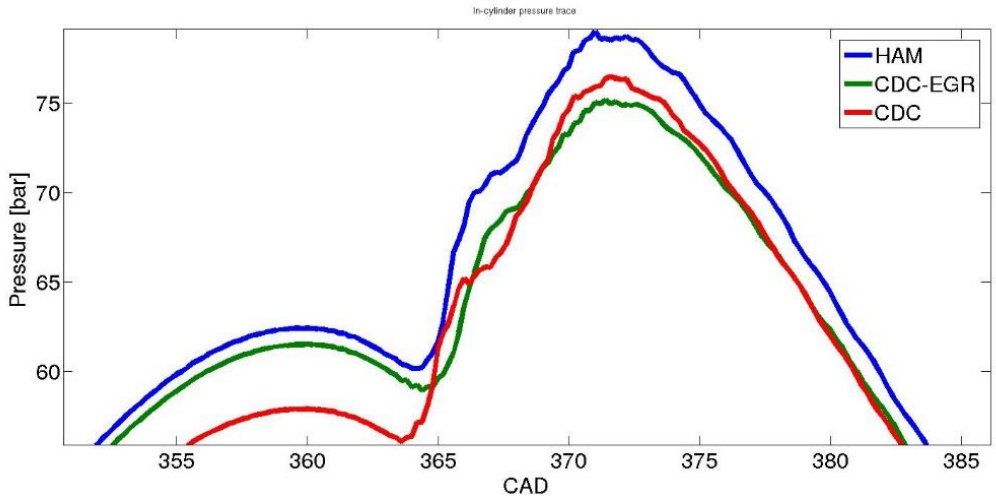

Figure 5.21 In-cylinder peak pressures as a function of crank angle at the same operating conditions

Back to the HAM system. CA50 for the HAM system was almost the same as for CDC but the inlet pressure was much higher. By adding the water in to the cylinder, some parts of the combustion energy is converted from the form of heat to the form of pressure. Water droplets become vaporized by absorbing heat which promotes high pressure steam inside the cylinder [35]. It explains high peak pressure in the HAM setup.

5.5.2 Soot

Soot formation was highest in the CDC-EGR system as can be seen in Figure 5.22. Soot builds up at rich mixtures because of lack of oxygen. To explain why the HAM system had lower soot emissions then CDC, the oxygen available for the combustion has to be seen again. It can be seen table 5.1.The air flow for the HAM system was much higher than for CDC-EGR. It is also good to see figure 1.7 again, where the trade-off between NOx and soot is shown. It explains the result in figure 5.22.

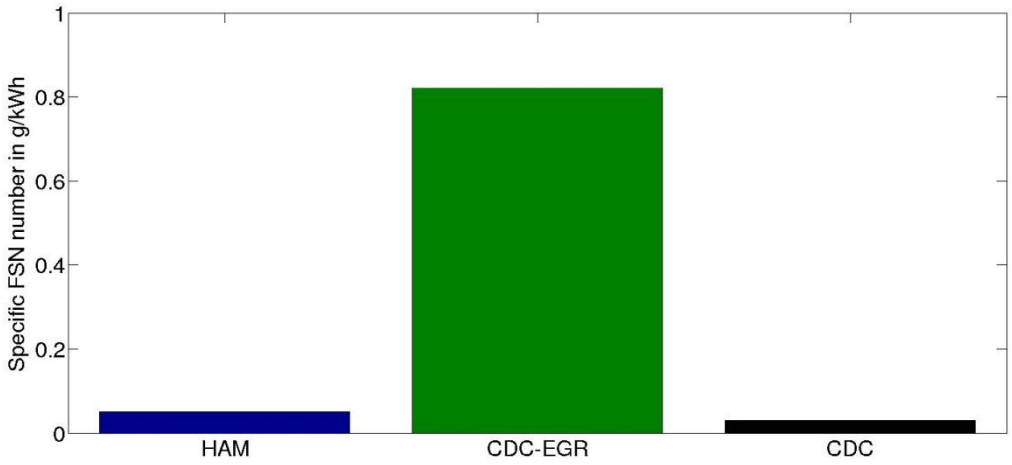

Figure 5.22 Specific soot for the different systems

5.5.3 HC

Hydrocarbon emissions can be seen in Figure 5.23. The HC emissions are the result of not fully combusted fuel. The CDC-EGR system had the lowest HC emissions because of higher in-cylinder peak temperature and the lowest amount of fuel injected per cycle compared with the HAM system. Due to the highest in-cylinder peak temperature in the CDC setup, the HC emissions were lower in CDC compared with the HAM system.

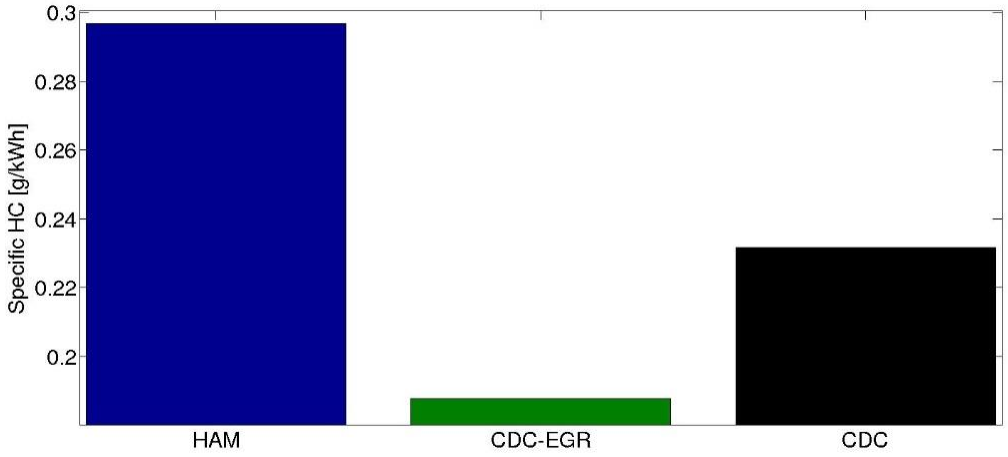

Figure 5.23 Specific HC for the different systems

5.5.4 CO

Carbon monoxide is not as harmful as NOx but still the CO emissions had to be investigated. Lambda is the most important parameter which directly affects the CO formation. Rich mixtures give high amount of CO. The lambda values for the systems can be seen in table 5.1. Figure 5.24 illustrates the CO emissions.

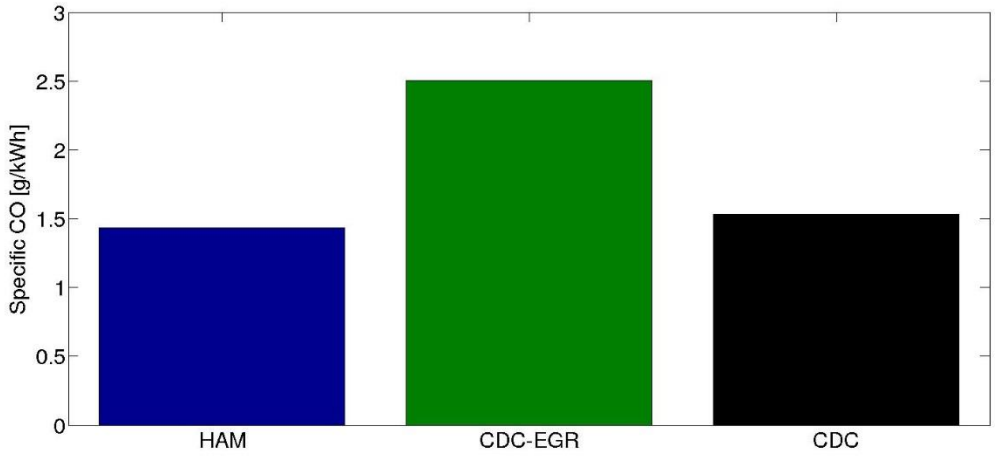

Figure 5.24 Specific HC for the different systems

5.5.5 CO_2

Comparison of the CO_2 emissions gave the following result. Due to the higher access of air, the HAM setup had little bit higher CO_2 emissions compared with the CDC-EGR system. Figure 5.25 illustrates this.

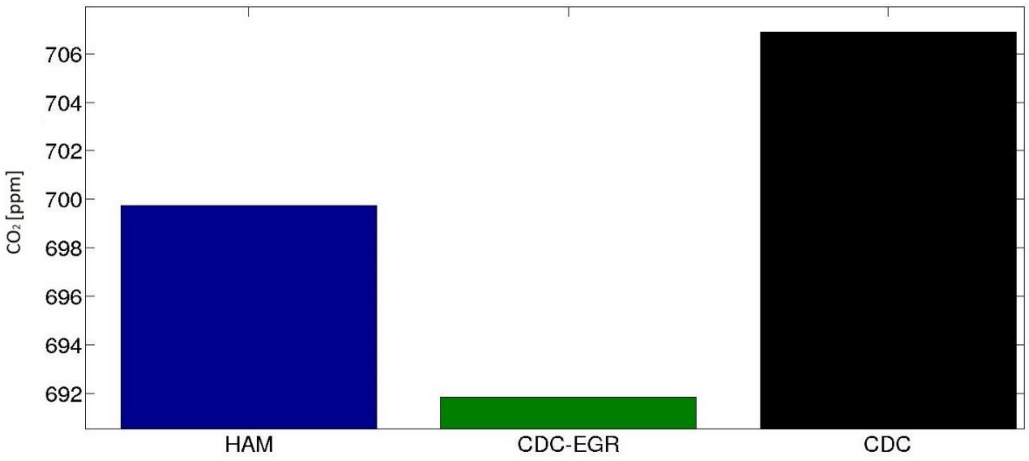

Figure 5.25 CO_2 for the different systems

5.6 Fuel consumption

Specific fuel consumption (*bsfc*) was higher for the HAM setup compared with CDC-EGR. The *bsfc* of the HAM system was 1.3 % higher, as shown in Figure 5.67. Different parameters such as the total efficiency and the heat losses played the beneficial role in the fuel consumption reduction. The same trend as in figure 5.26, can be seen in figure 5.9, where the total efficiency has been represented.

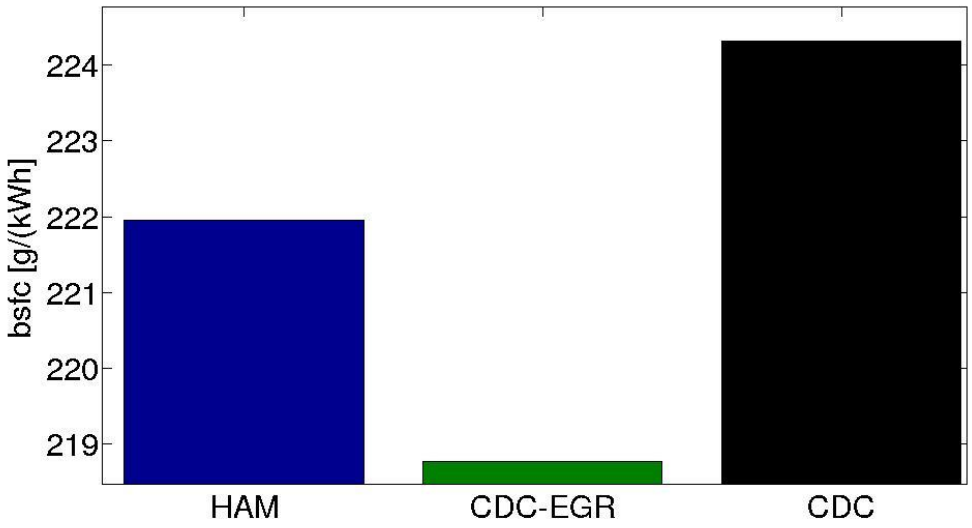

Figure 5.26 *bsfc* for the different systems

5.7 Water consumption and humidifier

The most crucial element in the HAM system was the amount of water that had been fed in to the cylinders. Calculation of how much water had been consumed by the engine gave the following result. It was consumed 16 grams water that equals 2.6 gram per cylinder. The relative humidity was 100% which was confirmed with amount of water flow. The water flow into the humidification tower was 162 g/s.

Figure 5.27 illustrates the amount of water injected per amount of fuel at different SOI. This value varies mainly because of the different fuel flow per cycle. In general, earlier SOI had positive effects on the fuel economy. CA50 for the HAM system was lower at earlier SOI.

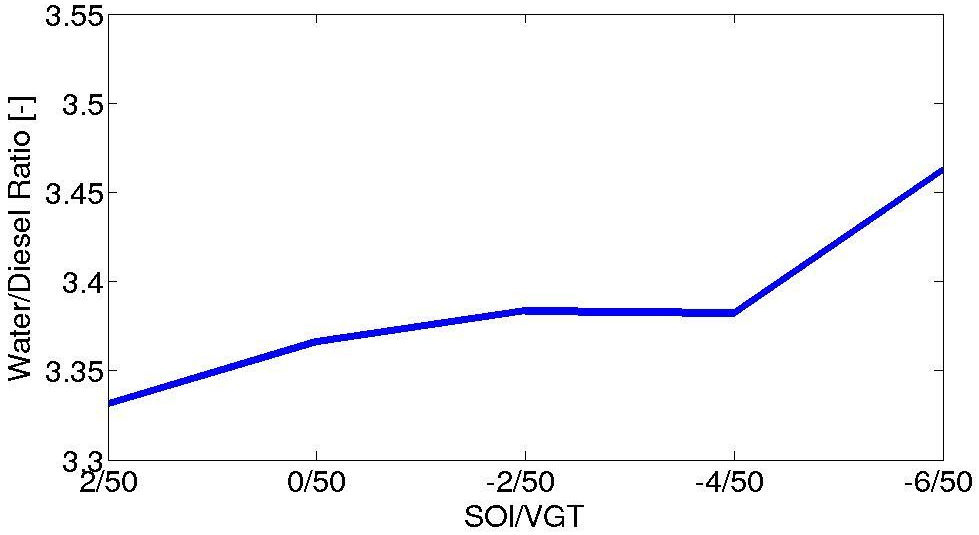

Figure 5.27 water/diesel ratio at different operating conditions

5.8 Sources of errors

There are many factors that could affect the experimental results. First of all, the systems were equipped with many sensors. These sensors could give an incorrect value. Several types of deviations could be also observed. For example: the sensitivity errors, the dynamic errors or random errors could occur. The estimation of the error variance gave the following result. Deviation for the temperature sensors could possibly be 1-2°. Deviation for the pressure sensors could vary between 0.1-0.2 bar.

The different efficiencies were calculated by using the formulas. Each value was rounded to three digit numbers. The estimated efficiency values were not 100 % correct. The estimation of the error could be in the range of 0.5-1 %.

Woschni's heat transfer model was used for the estimation of the in-cylinder heat losses. A 10 % error in the prediction of in-cylinder heat transfer affects the engine performance prediction in the order of 1 % [32]. The exhaust gas emissions measurements also have some deviations. The calibration of the emission systems plays the beneficial role in the emissions measurements. The estimation of the error could be in the range of 1 % to 2 %

Chapter 6

Conclusions and Future Work

A study of the HAM system performance at low engine speed and low load operating point A25 did not show significant improvement in the fuel consumption and emission reduction compared with CDC-EGR. Despite the fact that the system had much better performance than the CDC system, CDC has no use in the heavy duty truck industry and the focus lied on the comparison of the CDC-EGR setup and HAM.

The PMEP value for the HAM system was decreased by 8.8 %. By adding the water into the cylinders, it gave additional enthalpy to the turbine because of increased mass flow of humid air. In turn it also gave lower pumping losses. The gas exchange and the volumetric efficiencies were improved by 0.2 % and 30 %, respectively, compared with CDC-EGR. Still the total engine efficiency of HAM was 0.7 % lower. The thermodynamic efficiency was also decreased by 0.3 %.

Higher heat losses were investigated in the humidification tower compared with the EGR cooler. The losses at the exhaust were lower mainly because of the waste heat recovery. 67 % of the exhaust heat energy was used for warming up the water. The heat loss to the combustion chamber walls was 2.4 % lower. It could be explained by the fact that injected water absorbed large amounts of heat in the cylinders and it reduced the amount of energy absorbed into the cylinders walls. If the system would be operated at higher speeds, more water would be fed into the cylinders. In turn the losses to the walls would be reduced more.

The NOx emissions were 1.7 times higher compared with CDC-EGR. This occurred because a small amount of water was fed to the system. This water amount was not enough to absorb the heat in charge to reduce the peak temperature as much as EGR could. Water added to the system was directly dependent on the speed and the load. At higher speeds the HAM system will probably have much better NOx emission improvement due to higher amount of water which the air can hold.

The results from this thesis work show that the HAM system had less engine performance at operating point A25. Simulations in the GT-Power software gave the same result. The brake efficiency for the A25 operating point was also lower compared with CDC-EGR. HAM had very good potential at higher speeds according to the simulations. The results of the simulations are presented in Appendix A.

There was no improvement in specific fuel consumption, mainly due to the system being operated at low speed and low load. The amount of consumed water was too small. Future work is to operate the HAM system at different operating points. Higher speeds with variations in load would be of most interest.

Chapter 7

Appendix A

A.1 Thermodynamic modelling of humidification tower

As a first step in modelling of humidification tower saturation line for air was developed for different temperatures for a particular pressure level. Mass flow of water into the humidifier depends on the water temperature fed to the humidification tower. Mass flow of water, temperature and pressure of air were logged using a logger. Saturation line will vary at different operating points of engine. It depends on the inlet pressure of air. The saturation pressure of air and the vapor enthalpy at different temperatures (1:100 degree) was calculated.

The enthalpy of the incoming air for the given pressure (pressure at each reference point) and temperature was calculated. The atmospheric air pressure was treated as an ideal-gas mixture. It can be found us the sum of the partial pressure of dry air P_a and that of the water vapor P_v.

$$P = P_a + P_v \ \ (kPa) \tag{A.1}$$

The specific humidity was calculated using $\omega = 0.662 P_v / (P - P_v)$ (kg water vapor per kg dry air)
The specific humidity shows the amount of water vapor present in a unit of dry air. The total enthalpy of atmospheric air is the sum of the enthalpies of the dry air and the water vapor:

$$h = h_a + \omega h_g \ \ (\frac{kJ}{kg} \text{dry air}) \tag{A.2}$$

The enthalpy of atmospheric air is expressed per unit mass of dry air. The enthalpy of water vapor in air can be taken to be equal to the enthalpy of the saturated vapor at the same temperature.

$$h_v(T, \text{low } P) \cong h_g(T) \tag{A.3}$$

Now the saturation line for air can be developed. Figure xx represent schematic saturation line for air there the temperature of saturated air can be found for any given inlet air enthalpy.

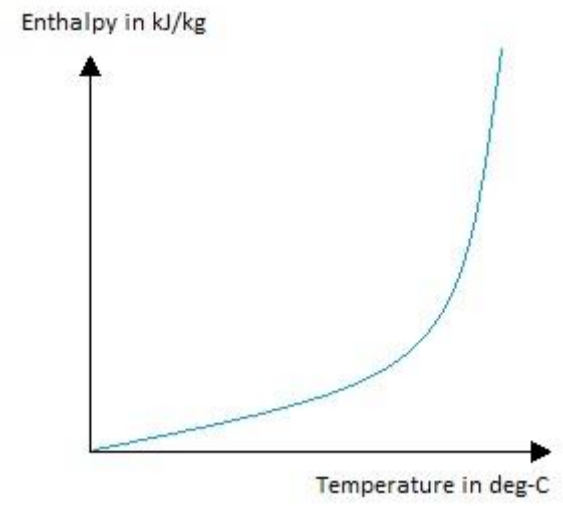

Figure A.1 Schematic saturation line for air

The water outlet temperature was assumed by adding the Pinch point (5˚) to the saturated air temperature for any given inlet air enthalpy. $T_{water\ out} = 5 + T_{sat,air\ in}$. Just to remind the pinch point was the temperature between the water outlet from the humidification tower and saturated airline corresponding to the enthalpy of compressed dry air at inlet in to the humidification tower.

The additional mass flow of water to the air was calculated using iterative approach. Few assumptions have been made to facilitate better understanding of the calculation process:

Air inlet:
Assumed, the partial pressure of vapor was 0 and $P = P_a$. Enthalpy of air at inlet could be found by the state file by using the P_{in} and T_{in}.

Water inlet:
Mass flow of water, temperature and pressure was known and thus the enthalpy was calculated. Water inlet in to the humidification tower was constant at 90˚. It is important to know that inlet water temperature should not be lower than air saturation temperature because if it is lower, this would result in water absorbing the enthalpy rather than giving it to the air.

Water outlet:
Water temperature out was calculated with Pinch point as it was mentioned before. It was assumed that there was no mass flow loss then the water is added to the air. The difference of enthalpy inlet and outlet of water was fed to the air. Flowing parameters have had to be finding in case to calculate the water vapor added to the air:

To calculate the mass flow evaporated, the specific humidity had to be known. Outlet temperature of air which depended on the mass flow of vapor added, had to be calculated for finding to the specific humidity. Residual iteration method was needed to calculate mass flow of air and the outlet temperature of water and air. Following steps was performed:

- Assumed the temperature of air out
- Assumed additional water flow to the air
- Temperature of water out is $T_{water\ out} = 5 + T_{sat,air\ in}$
- Calculated the enthalpy of water out. $P_{water\ in} = P_{water\ out}$
- The saturation pressure of water at assumed temperature of air out is calculated. Since the water vapor is 100 % humid, it is considered to be the water's saturation pressure instead of

vapor.

- Calculated the specific humidity of the humid air (omega). There $P_v = P_g$
- Calculated the mass of humid air added. Mass of humid air added = mass flow of air in multiplied by specific humidity of air
- Calculated the enthalpy of humid air, $h_{humid\ air} = (\dot{Q}_{air\ in} + \dot{Q}_{water\ in} - \dot{Q}_{water\ out})/\dot{m}_{air\ in}$
- The temperature of air outlet can be found with the vapor saturation curve which has already been calculated.
- This air outlet temperature and additional mass flow of humid air have to be used in first two steps until the result converge.

A.2 GT-Power simulations

Figure A.2 shows the results from the GT-Power simulations at different operating points. In those simulations the HAM setup has been tested with and without EGR. As it can be seen in the figure, the HAM system has very good potential at higher speeds while the A25 operation point did show any improvement.

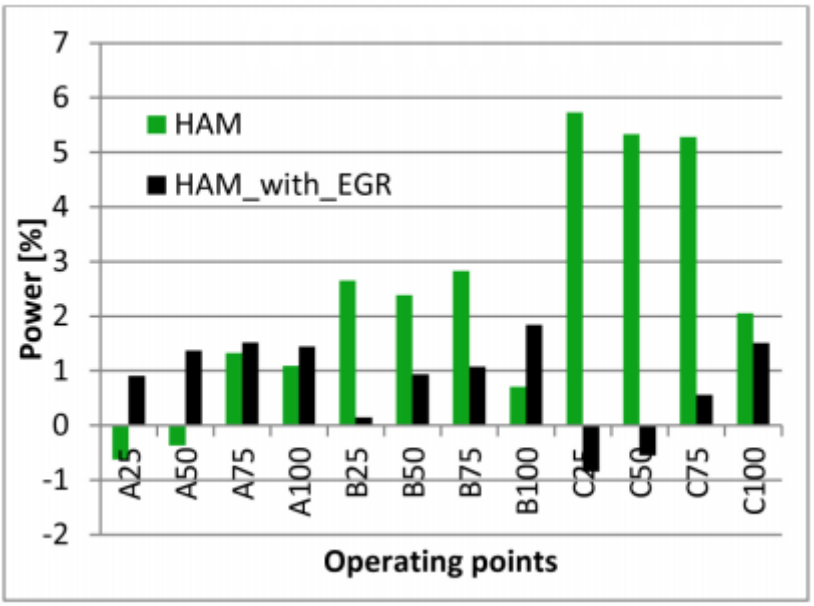

Figure A.2 Results of the simulations in GT-Power

Chapter 8

Bibliography

[1] “Evolution of the Internal-Combustion Engine,” Infoplease, [Online]. Available: http://www.infoplease.com/encyclopedia/science/internal-combustion-engine-evolution-internal-combustion-engine.html

[2] “Rudolf Diesel,” About.com, [Online]. Available: http://inventors.about.com/library/inventors/bldiesel.htm

[3] Automobile History,” About.com, [Online]. Available: http://inventors.about.com/od/cstartinventions/a/Car_History.htm

[4] Transportsektorns energianvänding, [Online]. Available: http://www.energimyndigheten.se/Global/Statistik/Transportsektorns_energianvandning_2012.pdf

[5] “Energy use in Sweden,” Sweden.se, [Online]. Available: https://sweden.se/society/energy-use-in-sweden/

[6] Dr. Ing. Nor bert Metz, World Wide Emission Trend 1950 to 2050, [Online]. Available: http://www.eurochamp.org/datapool/page/28/Metz.pdf

[7] “Priser & skatter,” SPBI, [Online], Available: http://spbi.se/statistik/priser/

[8] Introduction to Diesel Engines, [Online]. Available: http://www.gw.com/pdf/sampchap/9781590707708_ch01.pdf

[9] Siebers, D.L. and Higgins, B., “Flame Lift-Off on Direct-Injection Diesel Sprays Under Quiescent Conditions”, SAE paper 2001-01-0530, 2001

[10] “Internal-combustion engine: four-stroke cycle,” Britannica kids, [Online]. Available: http://kids.britannica.com/comptons/art-89315/An-internal-combustion-engine-goes-through-four-strokes-intake-compression%20bild%201.3

[11] B. Johansson, P. Tunestål, Ö. Andersson och M. Tunér, Combustion Engines Volume 1, Lund: Lund University, 2014.

[12] Heywood, J. Internal Combustion Engine Fundamentals. McGraw-Hill, New York, NY, 1988.

[13] Average In-Use Emissions from Heavy-Duty Trucks, [Online]. Available: http://www.epa.gov/otaq/consumer/420f08027.pdf

[14] Utsläpp och halter av kväveoxider och kvävedioxid på Hornsgatan, [Online]. Available: http://slb.nu/slb/rapporter/pdf8/slb2010_007.pdf

[15] “What Are Diesel Emissions,” DieselNet, [Online]. Available: https://www.dieselnet.com/tech/emi_intro.php

[16] Dalili, F., “Humidification in Evaporative Power Cycles”. Doctoral Thesis, Royal Institute of Technology Stockholm, Sweden, 2003

[17] B. Nemser, A. Stuart, “Reduced NOx/Hydrocarbon Emissions via Oxygen Enriched Lean Burn Engines”, EPA, 2000

[18] “Particulate Matter,” EPA, [Online]. Available: http://www.epa.gov/pm/

[19] Niklas Nordin, Introduction to Combustion in Diesel Engines, [Online]. Available: http://files.nequam.se/greenCarLecture.pdf

[20] Innovative Membrane Technologies for Reducing NOx Emissions and Preventing Transformer Failures, [Online]. Available: http://www.epa.gov/ncer/sbir/success/pdf/cms.pdf

[21] Z. Bazari, B.A. French: “Performance and Emissions Trade-Offs for a HSDI Diesel Engine - An Optimization Study”, SAE 930592

[22] “Cars and Light Trucks,” DieselNet, [Online]. Available: https://www.dieselnet.com/standards/eu/ld.php

[23] NOx Reduction after Retrofit of HAM System, [Online]. Available: http://cleantech.cnss.no/wp-content/uploads/2011/06/2010-MAN-Diesel-Turbo-61.3-NOx-reduction-after-retrofit-of-HAM-system.pdf

[24] Nord, K., Haupt, D., and Egebäck, K. “Particles and Emissions from a Diesel Engine Equipped with a Humid Air Motor System”, Luleå University of Technology, Division of Environment Technology, 2001

[25] Y. A. Cengel and M. A. Boles, “Thermodynamics - An Engineering Approach”, Third Edition, New Jersey: McGraw-Hill, 1998

[26] Narayanan, P., ”System Simulations to Evaluate the Potential Efficiency of Humid Air Motors”. SAE paper , 0148-7191, 2013

[27] “Humid Air Motors (HAM),” CNSS, [Online]. Available: http://cleantech.cnss.no/air-pollutant-tech/nox/humid-air-motors-ham/

[28] Miller, R., Davis, G., Lavoie, G., Newman, C. et al., "A Super-Extended Zel'dovich Mechanism for Nox Modeling and Engine Calibration," SAE 980781, 1998.

[29] “Emission Test Cycles,” DieselNet, [Online]. Available: https://www.dieselnet.com/standards/cycles/nte.php

[30] Dec, J.E., ”A Conceptual Model of DI Diesel Combustion Based on Laser-Sheet Imaging”, presented at SAE World Congress, 970873, 1997

[31] Haoyue, Z., Bohac, S., and Assanis, N., “Defeat of the Soot/NOx Trade-off Using Biodiesel-Ethanol in a Moderate Exhaust Gas Recirculation Premixed Low-Temperature Combustion Mode”, SAE 4024380, 2013

[32] R.,Rajput, “Internal Combustion Engines”, India, 1944

[33] B. Johansson, “Förbränningsmotorer”, Lund: Division of Combustion Engines, LTH, 2006

[34] A. Håkansson, “CA50 Estimation on HCCI Engine using Engine Speed Variations, Lund: Division of Combustion Engines”, LTH, 2007

[35] G. Tang, “Effect of Pressure Gradient and Initial Water Saturation on Water Injection in Water-Wet and Mixed-Wet Fractured Porous Media”, SPE Reservoir Evaluation & Engineering, 2011